Delft University of Technology

Document Version
Final published version

Licence
CC BY

Citation (APA)
Nalam, A., Mertens, M., Grewe, V., van Caspel, W., Jonson, J. E., & Butler, T. (2026). Understanding the effect of international ship NO_x emissions on surface O_3 concentration using three different attribution approaches. *Atmospheric Environment*, *384*, Article 122328. https://doi.org/10.1016/j.atmosenv.2026.122328

Important note
To cite this publication, please use the final published version (if applicable).
Please check the document version above.

Copyright
In case the licence states "Dutch Copyright Act (Article 25fa)", this publication was made available Green Open Access via the TU Delft Institutional Repository pursuant to Dutch Copyright Act (Article 25fa, the Taverne amendment). This provision does not affect copyright ownership.
Unless copyright is transferred by contract or statute, it remains with the copyright holder.

Sharing and reuse
Other than for strictly personal use, it is not permitted to download, forward or distribute the text or part of it, without the consent of the author(s) and/or copyright holder(s), unless the work is under an open content license such as Creative Commons.

Takedown policy
Please contact us and provide details if you believe this document breaches copyrights.
We will remove access to the work immediately and investigate your claim.

This work is downloaded from Delft University of Technology.

Atmospheric Environment 384 (2026) 122328

Contents lists available at ScienceDirect

Atmospheric Environment

journal homepage: www.elsevier.com/locate/atmosenv

Understanding the effect of international ship NO_x emissions on surface O_3 concentration using three different attribution approaches

Aditya Nalam [a,b,*,1], Mariano Mertens [c,d], Volker Grewe [c,d], Willem van Caspel [e], Jan Eiof Jonson [e,2], Tim Butler [a,b]

[a] Freie Universitaet Berlin, Berlin, Germany
[b] Research Institute for Sustainability at GFZ Helmholtz Centre for Geosciences, Potsdam, Germany
[c] Deutsches Zentrum für Luft- und Raumfahrt, Institut für Physik der Atmosphäre, Oberpfaffenhofen, Germany
[d] Faculty of Aerospace Engineering, Section Operations and Environment, Delft University of Technology, Delft, 2629HS, the Netherlands
[e] Climate Modelling and Air Pollution Division, Research and Development Department, Norwegian Meteorological Institute (MET Norway), PO 43 Blindern, Oslo, 0313, Norway

HIGHLIGHTS

- International shipping accounts for ~10-20 % of global anthropogenic NOx emissions.
- We use attribution approaches to quantify effect of these emissions on surface ozone.
- Emission-tagged approaches attribute 5-15 % ozone over select land regions to ships.
- O_3 response to ship NOx perturbation is ~2.3 %, is smaller than tagged contribution.
- This is due to a compensating negative response from non-ship emission contributors.

ABSTRACT

We use global atmospheric chemistry models (GACMs) to understand the extent to which NOx emissions from ships affect the surface ozone concentration and its seasonal cycle over continental regions. Here we use three different attribution approaches: NOx-tagged, combined-tagged and perturbation; implemented in three different GACMs, for understanding the qualitative and quantitative differences in employing these approaches for attributing surface ozone to NOx emitted from ships sailing over various marine regions. Using the NOx-tagged method, we attribute ~10 % contribution of ship NOx emissions to the simulated surface ozone over the receptor regions considered in our study. The summer peak in this contribution (eg. Over NW Europe) was mainly from NOx emissions over nearby marine regions (such as Baltic and North Seas). During the non-summer months, we simulate large contributions to surface ozone from remote marine regions (such as North Pacific). The combined-tagged approach attributes only ~7.7 % relative contribution from ship-tagged component, which is a smaller relative contribution compared to the NOx-tagged approach, due to the attribution considering an equally weighted small contribution of reactive carbon emitted from ships. Perturbation approach simulates the impact of changing NO_x emissions on surface ozone concentration, which in our study is ~2.3 % of the ozone in the unperturbed simulation. This impact simulated using the perturbation approach is smaller compared to the contributions simulated using the tagging approaches discussed above. We explore the reason for the smaller impact simulated using the perturbation approach compared to the tagged contributions, by simulating NOx-tagged and combined-tagged perturbations in ship NOx emissions and quantify the role of both perturbed and unperturbed tagged emission sources in contributing to the response to perturbation. The non-tagged surface ozone response to ship-NOx perturbation is ~2.5-5 times smaller than the response from the ship-tagged ozone component, because of compensating negative responses due to reduction in ozone production from other contributing tagged-components such as land-based natural and anthropogenic ozone precursor NOx sources.

1. Introduction

Maritime transport over open ocean waters typically involves usage of low-quality fuel, which along with the ship's engine design results in large emissions of air pollutants such as sulfur oxides, carbon monoxide, nitrogen oxides (NO and NO_2; collectively NOx), non-methane volatile

* Corresponding author. Institute of Meteorology, Carl-Heinrich-Becker-Weg 6-10, 12165, Freie Universitaet Berlin, Berlin, Germany.
E-mail address: adinalam@zedat.fu-berlin.de (A. Nalam).
[1] Now at Department of Atmospheric Physics, Faculty of Mathematics and Physics, Charles University, Prague, V Holešovičkách 2, 18,000 Prague 8, Czechia.
[2] Now retired.

https://doi.org/10.1016/j.atmosenv.2026.122328
Received 19 March 2026; Received in revised form 16 August 2026; Accepted 25 August 2026
Available online 26 August 2026
1352-2310/© 2026 The Authors. Published by Elsevier Ltd. This is an open access article under the CC BY license (http://creativecommons.org/licenses/by/4.0/).

organic compounds (NMVOCs) etc. Specifically, low quality fuel might lead to incomplete combustion and soot formation, the sulfur content in the fuel determines the sulfur oxide emissions, and the ship engine-type, which set the operating combustion temperature, determines the NOx emissions. The NOx emission from international shipping is notably large, accounting for ~10-20 % of global anthropogenic NOx emissions (Lawrence and Crutzen, 1999; Wang et al., 2023) and leads to formation of secondary pollutants such as tropospheric ozone and particulate matter. We focus our study on the concentrations of tropospheric ozone over land regions that stems from the emissions of NOx from shipping over open oceans (not inland waterways). Initially thought to be mostly of stratospheric origin (Junge, 1962), tropospheric ozone is a secondary pollutant produced from the reaction between ozone precursor gases: NOx and oxidized Reactive Carbon (RC: CH_4, CO and NMVOCs; Levy, 1972; Chameides and Walker, 1973; Crutzen, 1974). While NMVOCs are also a precursor to tropospheric ozone, ships emit a very small amount (~4 % of global anthropogenic NMVOCs; McDuffie et al., 2020). Therefore, most of the RC for tropospheric ozone formation from emitted ship NOx is from oxidation of methane, which is a well-mixed gas, also available in remote regions such as the open oceans (Butler et al., 2020; Holmes et al., 2014). The chemistry occurring within the expanding plume emitted by ships is not considered in our coarse-resolution model, leading to an instantaneous dilution of emitted NO_x into the large grid cells (Huszar et al., 2010; Vinken et al., 2011) of global atmospheric chemistry models (GACMs). This results in the simulated ozone production from ship NO_x more efficient than observed (Kim et al., 2016), thus making the modelling of ship NOx and its effects to be a challenging problem.

Exposure to large concentration of ground level ozone leads to several respiratory illnesses (Malashock et al., 2022) and crop losses (Avnery et al., 2011), while ozone in the free troposphere acts as a major greenhouse gas (Wang et al., 2022). Due to its large lifetime of up to a few weeks in the free troposphere, ozone can be transported across intercontinental distances (e.g., Huntrieser et al., 2005), thus making the study of trans-boundary effects of tropospheric ozone important for scientists and policymakers concerned with air quality (Franciscus et al., 2011). These trans-boundary effects are studied by establishing source-receptor relationships (SRRs): the extent to which the ozone precursor emission from a given source affects the ozone concentration over a given receptor region. This involves attributing the amount of ozone concentration at the receptor regions to precursor emissions from various sources, using various modelling approaches. In our study, we attempt to establish trans-boundary SRRs for ship NOx emissions (remote source) and continental regions (receptor) by attributing surface ozone concentration over 10 receptor regions in the northern hemisphere (will be explained in greater detail in section 2) to ship NOx emitted from various marine regions. Our study especially considers emission control areas (ECAs) as dedicated source regions to which the surface ozone is attributed. ECAs are ocean regions which typically extend a few hundred kilometers away from the coastlines of North America and Europe, defined by Marine Pollution Annex VI (MARPOL; IMO, 2008) intended to improve coastal air quality. By explicitly attributing continental surface ozone concentrations to NO_x emissions from ECAs and open ocean basins, we will be able to demarcate and comment on the exclusive influence of marine regions close to the coastline (such as ECAs), on surface ozone over land regions.

Typically, two methods/attribution approaches are used to establish SRRs using chemistry-climate models/atmospheric models involving atmospheric chemistry:

(i) Tagging: to calculate the absolute/relative *contribution* from a given precursor emission source to the ozone concentration over the receptor region.
(ii) Perturbation: to calculate the *impact* of changes in the ozone precursor emissions from a given source and assess the sensitivity of ozone concentration over any given receptor region.

The Tagging method involves simulating additional output variables of ozone molecules with labels of their precursor molecule emission sources. The sum of the tagged ozone molecules is equal to the total ozone that would otherwise be simulated in a non-tagged simulation, thereby delivering the exact contribution from the tagged emission source to the simulated ozone concentration. Since two precursor molecules are involved in forming one ozone molecule: NOx and RC, various approaches have been taken to label the simulated ozone to its precursor emission source (see Butler et al., 2018 for a comprehensive review of the tagging methods). Previous global modelling studies tag the ozone molecules for their NOx and RC precursor emission sources either in separate simulations: NOx-tagged and RC-tagged simulations (Butler et al., 2018), or within a single simulation: using a "combined-tagging" approach by giving equal weight to the proportion of tagged NOx and RC from a tagged emission source (Grewe et al., 2017; Rieger et al., 2018).

In our study, we perform the NOx-tagged simulation to attribute the surface ozone to ship NOx from various marine regions and to other tagged NOx emission sources. Here, the chemical mechanism in the model is modified to include additional tagged reactions that carry the tag of the emitted NOx molecule to the subsequent chemical species in the reaction pathway that eventually simulate tagged ozone. The tagged ozone simulated in the NOx-tagged simulation thereby conveys information on the contribution from the NOx source only, irrespective of which source the RC is emitted from, to produce the simulated ozone molecule. Butler et al. (2020) show that over most receptor regions considered in their study, ship NOx contribution to surface ozone remains the largest among the extra-regional anthropogenic NOx contributions. In a recent study, Nalam et al. (2025) showed that ship NOx contributions to global mean surface ozone were particularly large over densely populated areas especially over coastlines, making the contribution comparable to that of the global population weighted mean. In these studies, the contribution of ship NOx emissions from the entire oceans was considered, while in our study we further investigate this by tagging individual marine regions. NOx-tagging approach was also used in a regional modelling study (Lupascu and Butler, 2019) and showed that the ship NOx emissions from the nearby marine regions such as Mediterranean Sea and Baltic Sea had a substantial contribution over several European receptor regions analysed in that study.

The combined-tagging approach, as noted above, calculates the production and loss rates of tagged ozone which indicates the contribution of both NOx and RC emission from any tagged emission source. This calculation involves giving equal weight to the proportion of the tagged NOx and RC components. Mertens et al. (2018) estimate ~6 % contribution (radiative forcing of ~62 mWm^{-2}) to tropospheric ozone burden from shipping emissions (both NOx and RC). Since the RC emissions from ships aren't substantial as mentioned above, and since equal weight is given to NOx and RC components, the contribution from the ship tagged ozone using this combined-tagging approach is expected to be smaller compared to that calculated using the NOx-tagged approach as discussed for example in Kilian et al. (2024).

The Perturbation method calculates the impact of emission changes and involves performing two simulations: BASE (a reference simulation with all emissions) and PERTURBED (simulation with changed emissions). The difference in the simulated surface ozone between the BASE and PERTURBED simulations at any given receptor region conveys the SRR which in this case is the impact of/sensitivity to emission changes at the source. As opposed to tagging which involves modifying the model chemical mechanism or implementing additional diagnostics to simulate the *contributions* of various tagged emission sectors in a single simulation, the perturbation approach doesn't require any modification in the chemical mechanism in both the BASE and PERTURBED simulations in order to calculate the *impact* of emission changes. Jonson et al. (2020) use the perturbation approach to assess the impact of shipping emission from both open ocean shipping and ECAs on surface ozone over Europe. They found that the NOx emission reductions from Mediterranean,

Baltic and North Seas lead to an increase in ozone over mainly coastal European regions, due to smaller ozone titration (i.e ozone destruction by reaction with NO to form NO_2 and eventually getting deposited) during non-summer months.

Essentially the Tagging and Perturbation approaches answer two different questions: Perturbation calculates the effect of emission changes, while Tagging decomposes the ozone budget into its contributing components for any given state of the atmosphere. The Perturbation approach is generally used to assess the effectiveness of mitigation measures (as they involve changes in emissions) and will be applicable for policy-relevant modelling. The tagging approach on the other hand calculates the contributions from tagged emission sources and can be used to identify which emissions sources to mitigate (Grewe et al., 2010, 2012). A hybrid approach involving the inclusion of tagged chemical species in the perturbation simulations would be effective in assessing the role of contributions from unmitigated emission sources on the overall response to mitigation measures. For example, Mertens et al. (2018) perform a perturbation simulation with 5 % reduction in ship emissions with ship-emission-tagged chemical species included. They found that in a NOx-saturated regime, the contribution from ship emission-tagged component to the surface ozone remains nearly unchanged, while the contributions from other tagged sources (such as industry and land transportation) would increase.

In our study, we perform simulations using three GACMs attributing surface ozone over 10 world regions to ship NOx emissions over various marine regions (summarized in section 2) using the NOx-tagging, combined-tagging and perturbation approaches. We further perform NOx-tagged and combined-tagged perturbation simulations with ship NOx emissions reduced by 15 % to simulate the responses from tagged ozone species. Using the model outputs by employing these methods, we discuss the following questions in this study: In section 3.1: (i) how much surface ozone (as a seasonal cycle) over continental regions can be attributed to emissions from Ship NOx? (ii) To what extent do the approaches considered in this study differ (both qualitatively and quantitatively) in their attribution of surface ozone to ship NOx? (iii) What are the relative roles of various marine region's (ECAs vs open oceans) ship emissions that the simulated ozone concentration is being attributed to?, in section 3.2: How can a blend of tagging and perturbation approaches be used to explain the role and behaviour of unmitigated emission sources in SRR of ozone? And in section 4 we summarize our results by discussing the applications, merits and trade-offs of the attribution approaches considered in our study, and some of the limitations in our study along with several future study possibilities.

2. Methods

2.1. Model and setup descriptions

We employ three different attribution approaches in three different GACMs: (i) NOx-tagging approach in Community Atmosphere Model with Chemistry (CAM-Chem), (ii) Combined-tagging approach in ECHAM-MESSy Atmospheric Chemistry (EMAC), and (iii) Perturbation approach in the European Monitoring and Evaluation Program (EMEP) model, in order to simulate surface ozone (or scaled responses in surface ozone) over selected continental receptor regions and attribute it to the NO_x emitted from international shipping in various marine source regions (See Table 1). While, the attribution methods and the simulations are described in section 2.2, this subsection will describe the models employed and their specific settings used for the simulations considered in our study. All three models performed simulations for the year 2010, used the ship-based ozone precursor emissions taken from CAMS-GLOB-SHIPv2.1 dataset (Jalkanen et al., 2016) and prescribed methane concentration of 1775 ppbv as a boundary condition. Other boundary conditions such as prescribed meteorology reanalysis datasets, land-based ozone precursor emissions etc are different in each of the models as described in the paragraphs below (Table 1). The simulated

Table 1
Overview of simulations performed in our study. See section 2.1 for the detailed methodology involved in each of these simulations and Table S1 for a summary of various notations used to express the simulated/derived attributed ozone used in our study.

Model name	NOx-tagging method	Combined-tagging method	Perturbation method
	CAM4-Chem	EMAC	EMEP
Resolution	1.9° lat x2.5° lon	2.8° lat X2.8° lon	0.5° lat X0.5° lon
Method summary	Butler et al. (2018)	Grewe et al. (2017) Rieger et al. (2018)	Jonson et al. 2018
O_3 attribution method description	**Direct attribution** to NOx emitted from tagged sectors/regions	Attributed to **both NOx and RC** from tagged sectors/regions	**Sensitivity/ impact** of **changes** in Ship emissions
BASE simulations: Name and description	**NOx-tag-Base**: Attributing O_3 to anthropogenic NO_x emissions from various marine and land regions (Fig. 1a and b), and from natural sources[a]	**Comb-tag-Base:** Same as NOx-tag-Base, but for both NOx and RC emissions from anthropogenic and natural sources[a]. Additionally, O_3 is also attributed to RC from CH_4 oxidation and NO_x from N_2O oxidation.	**No-tag-Base**: Base Simulation without tagged chemical mechanism included (Standard Setup)
PERTURBED simulations: Name and description	**NOx-tag-Ship:** Same as NOx-tag-Base but with Ship NO_x emissions at all marine regions set to 85 % of that set in the BASE simulation	**Comb-tag-Ship**: Same as NOx-tag-Ship simulation but with combined-tagging included	**No-tag-Ship**: Same as NOx-tag-Ship but without tagging (Standard Setup) **No-tag-MReg**[b]: Same as No-tag-Ship but for individual marine regions (MReg) shown in Fig. 1a.
Sensitivity simulations that exclude ShipNOx parameterization (see section 2.1.5)	None	None	**NoSNPm-Base:** Same as NO-Tag-Base; ShipNOx parameterization excluded **NoSNPm-Ship**: Same as NO-Tag-Ship; ShipNOx parameterization excluded
Boundary conditions: Meteorology and ozone precursor emissions			
Common conditions	All three models simulate year 2010 and use Ship-based O_3 precursor emissions from CAMS-GLOB-SHIP-v2.1 repository and prescribe CH4 concentration of 1775 ppbv (see section 2.1).		
Meteorology reanalysis dataset	MERRA 2	ERA-interim	IFSv2
Land-based anthropogenic emissions	CAMS-GLOB-ANT-v4.2	CAMS-GLOB-ANT-v4.2	ECLIPSEv6
Biomass burning	GFED-v3	GFED-v3	FINN
Soil NOx	Tilmes et al. (2015)	ONEMIS submodel (Kerkweg et al., 2006)	Online calculation
Biogenic RC	CAMS-GLOB-BIO-v3.0	ONEMIS submodel (Kerkweg et al., 2006)	Online calculation
Lightning NOx	Price parameterization	Parameterized following Grewe et al. (2001)	Online calculation

[a] Natural sources include biogenic and biomass burning emissions of precursors (NOx only for NOx-tag-Base and both NOx and RC for Comb-tag-Base simulation), lightning NOx and ozone influx from stratosphere.
[b] Involves multiple PERTURBED simulations, each involving 15 % emission reduction over an individual marine region specified in Fig. 1a.

ozone concentration is attributed (using the methods described in subsection 2.2) to ship NOx emitted over several marine regions (see Table 2 and section 2.3 for further details). While the simulations using the EMEP model are performed by perturbing NOx emissions over individual marine regions, we also perform additional simulations in all three models with NOx emission perturbation over all marine regions simultaneously, described in section 2.2.4.

2.1.1. CAM-chem model

We use the NOx-tagging method of source attribution called TOAST (Butler et al., 2018) in CAM-Chem chemistry climate model at a resolution of 1.9° latitude x 2.5° longitude. CAM-Chem is run in a specified dynamics mode with meteorological fields taken from MERRA2 reanalysis (Molod et al., 2015). The temperature, horizontal winds, and sensible and latent heat fluxes from MERRA2 reanalysis dataset are nudged every time step (30 min) by 10 % towards analysis fields (i.e., a 5 h Newtonian relaxation timescale for nudging). In this model configuration, we prescribe emissions of land-based anthropogenic emissions from CAMS-GLOB-ANT-v4.2 (Granier et al., 2019), biogenic RC emissions from CAMS-GLOB-BIO-v3.0 (Sindelarova et al., 2021), biomass burning emissions from Global fire emissions database (GFED-v3) inventory (van der Werf et al., 2010), and soil NOx emissions are described as in Tilmes et al. (2015). Lightning NOx emissions are calculated using the Price parameterization (Lamarque et al., 2012; Price and Rind, 1992). The stratospheric concentrations of NO_x, O_3, HNO_3, N_2O, CO, and CH_4, taken from WACCM6 ensemble member of CMIP6 ensemble, are prescribed as an upper boundary condition and are relaxed towards climatological values (Emmons et al., 2020). Simulations in this configuration were performed for 2 model years with annually repeating boundary conditions to attain spin-up (difference in the tagged stratospheric contribution to surface ozone between two consecutive Decembers should be less than 1 %; Butler et al., 2018), and the output form the last model year has been considered for analysis.

Table 2
Abbreviations of all the tags used in our study. The tagged land regions are provided in Fig. 1b but are discussed as local and remote land regions depending on the receptor region (Fig. 1c) over which the analysis is being done. See Fig. 1 for the geographical extent of all the tagged regions considered in our study.

Tag Abbreviation	Full Name	Remarks
TOT	Total	Sum of all tags (also equal to the ozone simulated without tagging)
AIR	Aircraft	
CH4[a]	Methane oxidation	Exclusive RC source
Tags related to Natural Sources		
NAT	Natural	All natural sources combined
BIO	Biogenic	
BMB	Biomass Burning	
LGT	Lightning NOx	Exclusive NOx source
STR	Stratospheric influx	Not attributed to any tropospheric precursor
Land-based Anthropogenic Sources		
LOC	Local Anthro.	Only the local anthropogenic tag considered
REM	Remote Anthro.	Only the local anthropogenic tag excluded
Marine regions[b]		
SHP	All marine regions	Ship emissions from all marine regions considered simultaneously
BNS	Baltic and North Seas	
ENA	Eastern North Atlantic	
MBC	Mediterranean, Black, Caspian	
NAL	North Atlantic	
IDO	Indian Ocean	
NAE	North American East Coast	
NAW	North American West Coast	
NPA	North Pacific	
SHO	Southern Hemisphere Ocean	
ARC	Arctic Ocean	

[a] These tags are only used in our Combined-tagged simulations.
[b] Marine region abbreviations are also applicable for the perturbation method discussed in sections 2.1.3 and 2.1.4.

2.1.2. EMAC model

We use the combined-tagging method as a submodel called TAGGING diagnostic package within the MESSy (Modular Earth Subsystem) included in the EMAC (European Centre for Medium-Range Weather Forecasts – Hamburg (ECHAM)/MESSy Atmospheric Chemistry) chemistry climate model at a resolution of 2.8° latitude x 2.8° longitude (Grewe et al., 2017; Mertens et al., 2018, Mertens et al., 2024 etc.). This model is run in a quasi-chemistry transport model mode (Deckert et al., 2011) where EMAC is nudged by Newtonian relaxation of temperature, divergence, and vorticity and the logarithm of surface pressure (Jöckel et al., 2006) towards ERA-Interim reanalysis data (Dee et al., 2011, Table 1) at every model time step. The simulations used in our study for year 2010 have been branched off from year 2009 (allowing one year of spin-up by 2010) of a previous transient simulation. The general model set-up is very similar as the specified dynamics simulation described by Jöckel et al. (2016). Similar to CAM-Chem, EMAC simulations have also used CAMS-GLOB-ANT-v4.2 and GFED-v3 for land-based anthropogenic and biomass burning emissions respectively. Soil NOx and biogenic isoprene emissions have been calculated online using ONEMIS submodel (Kerkweg et al., 2006) and lightning NOx emissions were parameterized as in Grewe et al. (2001).

2.1.3. EMEP model

The perturbation method for attributing surface ozone to changes in ship NOx emissions from individual marine regions has been used in the EMEP chemistry transport model (Jonson et al., 2020), at a resolution of 0.5° latitude x 0.5° longitude. In this model configuration, we use IFS re-analysis dataset (ECMWF, 2014) for the nudging of meteorological (dynamical and thermodynamical) fields. Land-based anthropogenic emissions are taken from ECLIPSEv6b (IIASA, 2019), and biomass burning from FINN (Wiedinmyer et al., 2023) inventories. Biogenic and lightning emissions are calculated online. The EMEP model has been used and developed for research and policy support purposes over the course of decades (Simpson et al., 2012). The version employed in the current work (rv5.5) uses the EmChem19 chemical mechanism (Bergström et al., 2022), which uses a simplified set of lumped VOC species to balance realism with computational complexity (Ge et al., 2024). Photochemical reactions are driven by online radiative transfer calculations made by Cloud-J v7.3 (van Caspel et al., 2023). Using this model, each simulation is preceded by a 6-month spinup period.

We analyse the seasonal cycle of surface ozone and its source attribution (NOx-tagged contribution, combined-tagged contribution, scaled responses to perturbation; see Table 2) over some select receptor regions in North America, Europe and East Asia (Fig. 1c). A description of the attribution methods, models used, simulations performed and the basis for the selection of the receptor regions are provided in the subsections below.

2.2. Attribution method description and terminology

This subsection explains the details of the simulations performed and the attribution methods used in them (see Table 1 for a concise overview). The ozone attributed to a given precursor source (listed in

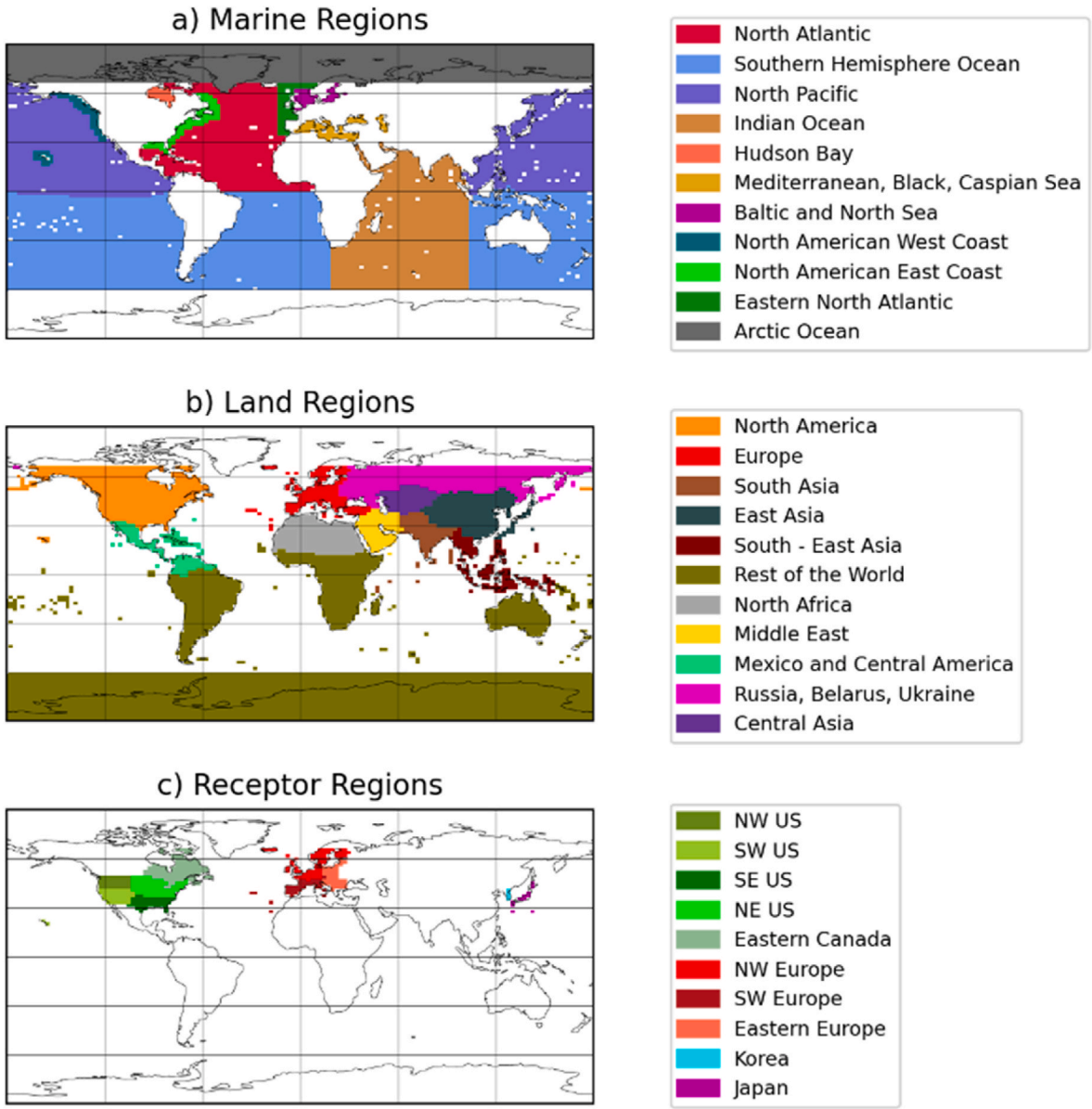

Fig. 1. a) Marine regions whose ship emissions to which our simulated ozone (see Table 1) is attributed. See Supplementary Fig. S1 for the magnitude of NOx emissions from these marine regions used in our study. b) Land regions whose anthropogenic precursor emissions to which ozone is attributed in our tagged simulations. Here we aggregate the tags as local/remote land regions based on the receptor region over which the model output is analysed. See supplement for the disaggregated contribution from these land regions. c) Receptor regions over which the simulated surface ozone is evaluated (section 2.2) and analysed (section 3) in our study.

Table 2) using each of the attribution methods is referred using the notations listed in Table 3.

2.2.1. NOx-tagging in CAM4-Chem

The NOx-tagging method involves simulating ozone molecules with labels containing the identity of their precursor NOx sources (also known as NOx-tags or simply Tags). This is achieved by modifying the existing chemical mechanism (MOZART-4; Emmons et al., 2012) by including additional reactions involving the "NOx-tagged" chemical species along with the standard reactions in the existing chemical mechanism. The simulated ozone and other associated molecules (e.g., NO_2, N_2O_5 etc.) are labelled with the source identity of the molecules' emitted NOx precursor source identity (also known as TAG; see Table 2 for the full list of tags in this study), irrespective of where the RC precursor comes from to produce the molecule. In CAM4-Chem, we use the implementation of this method that was first demonstrated by Butler et al. (2018) and was used in a few other studies hence (e.g. Butler et al., 2020; Li et al., 2023; Nalam et al., 2025 etc.). A brief illustration of this method is explained below.

Tropospheric O_3 formation occurs due to the reaction of emitted primary pollutants: NO and RO2 (HO2 and oxidized RCs combined), forming NO_2 and eventually photo-dissociating to produce odd oxygen atoms and finally ozone as illustrated in the following reactions:

$$NO + RO_2 \square NO_2 + Products \quad \text{(R1)}$$

$$NO_2 \xrightarrow[O_2]{h\nu} O_3 + NO \quad \text{(R2)}$$

Apart from the oxidation of NO with RO_2, NO_2 is also formed via the O_3-NO_x null cycle, especially in environments polluted with large NO_x concentration, via the reaction:

$$NO + O_3 \rightarrow NO_2 \quad \text{(R3)}$$

Table 3
Summary of various notations used to express the simulated/derived surface ozone attributed through either tagging or perturbation methods used in our study.

Notation	Nomenclature	Description
$O_3^{TAG(NOxT)}$	NOx-tagged *contribution*	NOx-tagged Ozone attributed to NO_x from a given source (TAG) in our NOx-tag-Base simulation, simulated using reactions R4-R6
$O_3^{TAG(Comb)}$	Combined-tagged *contribution*	Comb-tagged Ozone attributed to both NO_x and RC from a given source (TAG) in our Comb-tag-Base simulation calculated through equation 1
$O_3^{MReg(Pert)}$	*Potential impact* or *scaled response* to ship NOx perturbation at MReg marine region	Ozone attributed to change in Ship NO_x emissions from 85 % to 100 % of the Base simulation from a given marine region (MReg; Fig. 1b) derived from equation 2
$O_3^{Ship(Pert)}$	*Potential impact* or *scaled response* to ship NOx perturbation over all marine regions at once	Ozone attributed to change in Ship NO_x emissions from 85 % to 100 % of the Base simulation from all marine regions, derived from equation (5).
$O_3^{TAG(Pert_NOxT)}$	*Scaled response* of NOx-tagged ozone components to ship NOx perturbation over all marine regions at once	Change in NOx-tagged ozone components due to increase in Ship NO_x emissions at all Marine regions, derived from equation (3).
$O_3^{TAG(Pert_Comb)}$	Same as above but for Combined-tagged ozone components.	Same as above but for Combined-tagged ozone components, derived from equation (4).

This reaction R3 is also called NO_x titration reaction which involves the destruction of O_3 while forming NO_2.

The above reactions are modelled in CAM4-Chem within the MOZART-4 standard chemical mechanism (Emmons et al., 2012). We add new NOx-tagged chemical reactions to the existing set of reactions modelled in the standard chemical mechanism. For example, the NOx-tagged equivalents of reactions R1 and R2 are expressed roughly as:

$$NO^{TAG(NOxT)} \xrightarrow{RO_2} NO_2^{TAG(NOxT)} \tag{R4}$$

$$\boldsymbol{NO_2^{TAG(NOxT)} \xrightarrow[O_2]{h\nu} O_3^{TAG(NOxT)} + NO^{TAG(NOxT)}} \tag{R5}$$

Here, TAG represents the source from which NO molecule is emitted. The resulting product of NO reacting with RO_2: NO_2 and subsequently the O_3 molecule (after photolysis) both hold the same TAG irrespective of the source of the RO_2 molecule participating in the reaction. The key takeaway is that the TAG held by the chemical species is carried over to other reactive molecules and is conserved as the reaction progresses. The NOx-tagged representation of R3 is slightly more complicated as it involves the reaction between NO and O_3 that could both carry a different tag and could lead to a tag overwriting problem and loss of tag identity while deciding which tag would the resulting NO_2 molecule inherit. Therefore, we implement the tagging using the chemical family concept where the chemical species involving the odd oxygen atoms (such as O_3, O1D, NO_2, NO_3 etc.) are treated as separately tagged species (see Supplementary Text S1 or Butler et al., 2018 for detailed explanation) thereby avoiding any loss of tag identity. Overall, we note that the sum of all individual tagged ozone tracers is equal to the total ozone simulated by the model with the standard chemical mechanism (without the involvement of tags). The tags considered in this simulation for our study are summarized in Table 2 and the region definitions for the marine and land-based anthropogenic emission tags are summarized in Fig. 1a and b. We perform the NOx-tag-Base and the NOx-tag-Ship simulations using this method (see Table 1 and section 2.2.4).

2.2.2. Combined-tagging in EMAC

This approach tags Ozone (as odd oxygen), Carbon monoxide, PAN, NO_y (chemical species that contain NO_x; eg., NO, NO_2, NO_3, N_2O_5, HNO_3 etc.), RCs, OH and HO_2 (the latter two in a steady state). The detailed description is given by Grewe et al. (2017); Rieger et al., 2018. Here, we describe the approach in a simplified manner, summarizing the tagged ozone production pathways via reactions of NO_y with RO2 (HO2 and oxidized RCs as defined in section 2.2.1).

In this approach, the instantaneous production rate of the tagged ozone molecules within every grid cell is calculated by weighting the chemical production rates, diagnosed while solving the atmospheric chemistry, via the ratio of the tagged NO_y and RO2 to the total mixing ratios of the untagged species. The production rate of O_3 attributed to a given precursor (both NOy and RO2) sector with its identity label "Tag" using the combined-tagging method is calculated as:

$$pO_3^{Tag(Comb)} = pO_3 * \frac{1}{2}\left(\frac{NO_y^{Tag(Comb)}}{NO_y} + \frac{RO_2^{Tag(Comb)}}{RO_2}\right) \tag{1}$$

Where "p" represents the production rate of the ozone variable, and "Tag (Comb)" refers to any of the tags modelled using the combined-tagging approach, summarized in Table 2. Here, the production rate of combined-tagged ozone is calculated as a fraction of the diagnosed ozone production rate. This fraction is calculated as a relative proportion of the instantaneous mixing ratio of tagged NO_y and tagged RO2 species. The tagged NO_y and RO2 species are given equal weights in reaction (R1) which leads to the factor of 0.5 in Equation (1). Note that since we also consider sources of RC in this approach, an additional tag for RC from methane oxidation ("CH4" tag; Table 2) has also been included.

The important difference to the NO_x tagging approach is, that the tagged ozone production is always attributed to NO_y and RO2 precursors from each source. Similar to the NOx-tagging approach, the tagged components derived using the combined-tagging method also add up to the total ozone simulated by the model without tagging. We perform the Comb-tag-Base and the Comb-tag-Ship simulations using this method (see Table 1 and section 2.2.4).

2.2.3. Perturbation in EMEP

This perturbation method can be used in any GACM, which unlike the tagging methods discussed above, do not strictly require any modifications to the standard chemical mechanism to output tagged chemical species. In our study, we perform perturbation simulations for attributing to individual marine region NOx emissions using the EMEP chemistry transport model (section 2.1.3). The method involves one BASE (e.g., No-Tag-Base) simulation as reference and several PERTURBED simulations (one for each marine region: No-Tag-Mreg) where the NOx emissions from a given marine region "MReg" are reduced by 15 % (Table 1). The resulting ozone attributed to international ship NOx emissions from that particular marine region "MReg" is calculated as:

$$O_3^{MReg(Pert)} = \left(O_3^{No-tag-Base} - O_3^{No-tag-MReg}\right) * \frac{100}{15} \tag{2}$$

where "Mreg" represents each of the marine regions summarized in Table 2 and Fig. 1a. Here we calculate the scaled response in the modelled surface ozone (also called potential impact (see Table 3); Clappier et al., 2022) to an increase in NOx emissions from 85 % (in PERTURBED (No-tag-Mreg) simulations) to 100 % (in BASE (No-tag-Base) simulation) ship NOx emitted in that particular marine region. In other words, the extent of perturbation in NOx emissions in our study is an increase of ~17.65 % relative to the PERTURBED simulation. The difference between the surface ozone simulated in the

BASE and PERTURBED simulations is then scaled by the perturbation factor (100/15 in our study), to calculate the scaled response.

Following Jonson et al., 2020, we implement a "ShipNOx" parameterization (SNPm; first introduced in Simpson et al., 2015) in the EMEP model simulations mentioned above. While it is known that instant dilution of NOx emissions into coarse grid cells leads to overestimation of ozone formation as noted earlier, SNPm splits 50 % of ship NOx emissions are into a pseudo-species whose only products involve the formation of HNO_3 (mimicking chemical conditions within the high-pollution environment of ship plumes). The presence and absence of SNPm in the simulation communicates the lower and upper limits of the effect of NOx emitted from ships on the simulated surface ozone. We perform additional sensitivity simulations that exclude SNPm: NoSNPm_Base and NoSNPm_Ship (see Table 1) and determine this upper limit. Further details and results related to the exclusion of SNPm are discussed in Appendix A1.

2.2.4. Additional global shipping perturbation simulation in all three models

Apart from the perturbation simulations for individual marine regions using the EMEP model as mentioned above, we also perform an additional perturbation simulation, where the NOx emissions from all the marine regions are together reduced to 85 % of the BASE. We perform this perturbation simulation in all the models considered in our study: EMEP (No-tag-Ship; NoSNPm-Ship), EMAC (Combined-tag-Ship) and CAM4-Chem (NOx-tag-Ship) (see Table 1). This additional simulation in EMAC and CAM4-Chem also includes the respectively modified tagged chemical mechanisms as summarized above. The inclusion of tagging in this perturbation simulation can help track the responses from various tagged components, enabling us to enhance our understanding of the compensating feedbacks happening due to the introduction of perturbation in emissions (Butler et al., 2020; Mertens et al., 2018).

We use the same prescribed meteorology and other boundary conditions (e.g., CH_4 concentration, land-based precursor emissions) as used in the BASE simulations in the respective models, for all our PERTURBED simulations (including the ones mentioned in section 2.2.3) to understand the exclusive effect of ship NOx emission perturbation. The modelled surface ozone response to this perturbation for both total surface ozone (that would also be simulated without tagging) or the individual ozone tags is calculated using equation (2), replacing the ozone variable with the total/tagged ozone variable simulated in the respective BASE and the all-marine-region ship perturbation simulation described in this section (see Table 3 for the notations). This calculation is shown for the NOx-tagged, Combined-tagged and non-tagged simulations respectively below:

$$\boldsymbol{O_3^{Tag(Pert_NOxT)}} = \left(\boldsymbol{O_3^{Tag(NOx-tag-Base)}} - \boldsymbol{O_3^{Tag(NOx-tag-Ship)}}\right) * \frac{\mathbf{100}}{\mathbf{15}} \quad (3)$$

$$\boldsymbol{O_3^{Tag(Pert_Comb)}} = \left(\boldsymbol{O_3^{Tag(Comb-tag-Base)}} - \boldsymbol{O_3^{Tag(Comb-tag-Ship)}}\right) * \frac{\mathbf{100}}{\mathbf{15}} \quad (4)$$

$$O_3^{Ship(Pert)} = \left(O_3^{No-tag-Base} - O_3^{No-tag-Ship}\right) * \frac{100}{15} \quad (5)$$

2.3. Ozone precursor emission sources for attribution

The main focus of our study is to attribute the simulated surface ozone to NOx emissions from shipping over marine regions as shown in Fig. 1a. These include smaller marine regions close to the European (Baltic and North Seas (BNS), Eastern North Atlantic (ENA) and Mediterranean, Black, Caspian Seas (MBC)) and North American (Hudson Bay (HBY), North America East (NAE) and West Coast (NAW)) coastlines (some of them are defined as ECAs in MARPOL recommendations; see Fig. 1 in Topic et al., 2023) and open ocean basins: Arctic (ARC), Indian (INO), North Atlantic (NAL), North Pacific (NPA), and Southern Hemisphere (SHO) ocean (see Table 2 for abbreviations and Fig. 1a for the map of these regions). The ARC "marine" region shown in Fig. 1a also covers land (due to Arctic region definition), nevertheless the NOx emission from ARC is very small as shown in the seasonal cycle of emissions from each of these marine regions provided in Fig. S1. The attribution of surface ozone to these marine regions is performed using all three methods (NOx-tagging, Combined-tagging and Perturbation) described above.

Additionally, our tagging simulations include simulating source-tagged ozone attributed also to non-marine sources such as land-based precursor emission sources and influx from stratosphere (STR). In case of NOx-tagged simulations, ozone is attributed only to the NOx emissions from various sources such as ship emissions from individual marine regions, land-based anthropogenic (categorized by continental region; see Fig. 1b), lightning (LGT), aircraft (AIR), biogenic emissions (BIO), and biomass burning (BMB). These source categories would be referred to as "tags" in our discussion. The Combined-tagged simulations attribute ozone to both NOx and RC emitted from the source tags mentioned above. Additionally, the combined-tagged simulations also attribute ozone to methane oxidation (CH4), which is a source of RC for ozone production.

As noted in the earlier subsections, the sum of all the tagged ozone components in any given simulation is equal to the total ozone that would otherwise be simulated without the inclusion of tagged chemical mechanism. Within these tagged simulations, we categorized the sum of individual marine region tags as total ship-tagged component "SHP". Similarly, sum of tags corresponding to natural sources such as STR, BIO, BMB and LGT would be categorized as natural sources (NAT), and the individual land-based regional anthropogenic components (see Fig. 1b for the tagged land regions) is categorized as remote (REM) and local (LOC) land-based anthropogenic components. The categorization for REM and LOC is done subjectively for each receptor region being considered. For example, in case of Japan as a receptor region, the LOC would be East Asia, while to sum of all other tagged regional anthropogenic sources: Europe, North America, South Asia etc. would be aggregated into the REM category. We express the tagged contributions in absolute mixing ratios (in ppb) and relative contributions to the total ozone from the tags in %.

2.4. Receptor regions and evaluation

We evaluate our simulated monthly mean surface ozone for the year 2010 from the BASE simulations of all three models against the gridded observation dataset from the tropospheric ozone assessment report (TOAR; Schultz et al., 2017) version 1. The gridded observations were made available by collecting observations from several rural measurement sites across the continents and compiling them into a single gridded dataset. We therefore evaluate our model output against observations only over the gridcells where the TOAR rural data is available following 10 receptor regions: North American regions include NW US, SW US, NE US, SE US, and Eastern Canada; European regions include NW Europe, SW Europe, Eastern Europe; and East Asian regions include Korea and Japan (Fig. 1c) as defined in Galmarini et al. (2017). The limited choice of regions for evaluation and analysis is due to the limited coverage of observation grid cells in the TOAR gridded dataset. Although, we evaluate the simulated ozone at these regions only over the grid cells where observation data is available, we analyse and discuss the monthly mean model results over the entire region in section 3. Since the gridded dataset is available at a resolution same as that used in CAM4-Chem model, we re-grid the model output from the other models to this resolution using a standard conservative re-gridding algorithm, for the sake of convenient evaluation of the simulated surface ozone.

In Fig. 2, we show the seasonal cycle of monthly regional mean observations over the regions considered in our study (black line) along with the surface ozone fields simulated in the BASE simulations of all models described in Table 1. The characteristic spring and summertime peak in surface ozone concentrations over nearly every region shown in the TOAR observations is simulated by all three models used in our

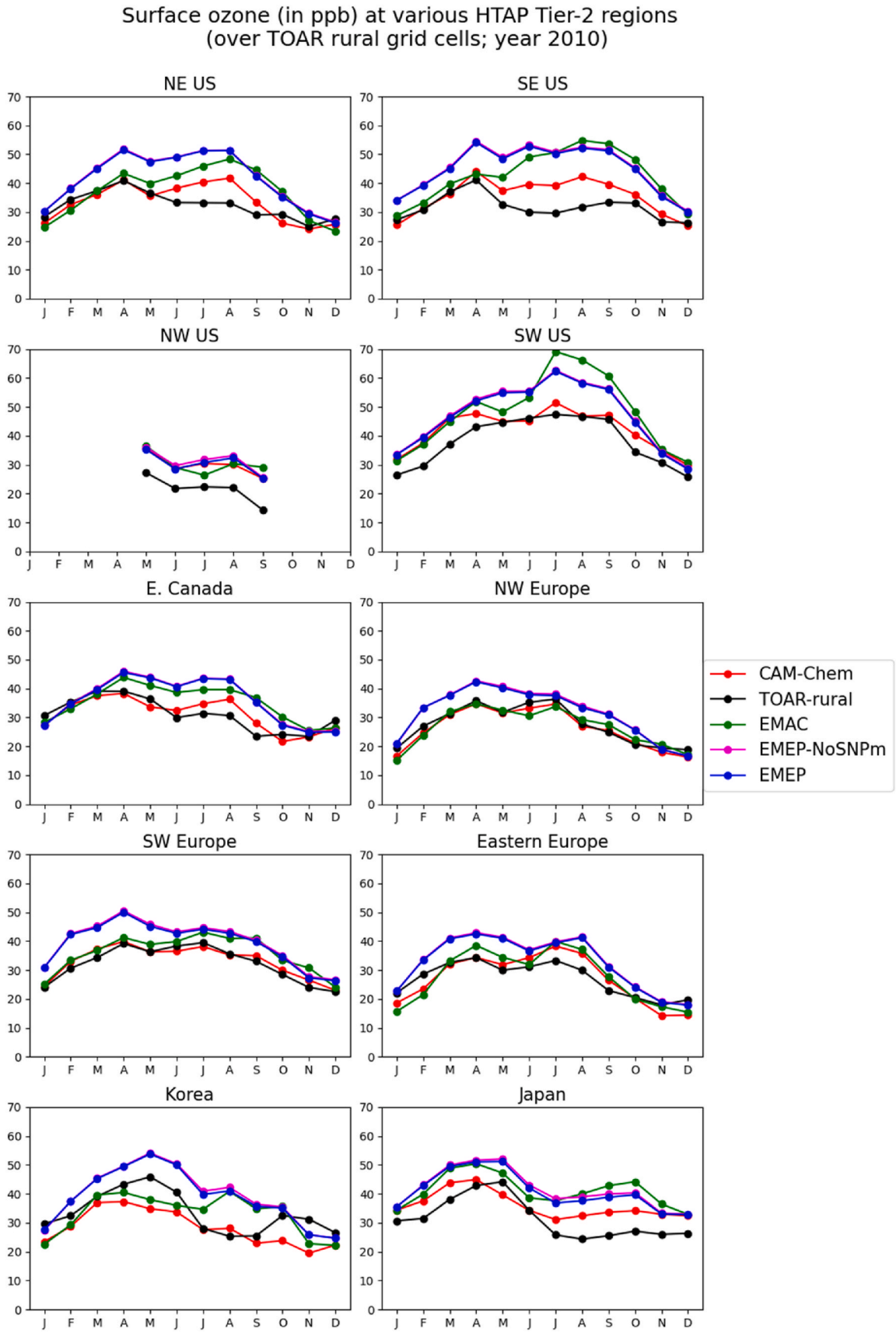

Fig. 2. Evaluation of surface ozone (in ppbv) simulated in the Base simulations (NOx-tag-Base (CESM; red), Comb-tag-Base (EMAC; green), No-tag-Base (EMEP; blue), and NoSNPm-Base (EMEP-NoSNPm; magenta)) of our study against gridded observations from TOAR dataset (rural only; black). Shown are the mean surface ozone fields over various HTAP Tier 2 regions and only over grid cells and during the months where/when the TOAR rural data is available. See Supplementary

Table TS1 for the number of grid cells in each receptor region and the number of grid cells where TOAR gridded rural monthly mean ozone mixing ratio data is provided.

study. The summertime peak is overestimated by ~5-15 ppbv over most of the regions by all the models used in this study. EMAC simulation (Combined-tag-Base) especially overestimates summertime peak over SW US by ~25 ppbv compared to observations. This overestimation is ~20 ppbv larger compared to the overestimation by other models in this study. Springtime peak is simulated well by all models over most regions with deviations from observations being within ~5 ppbv. The overestimation feature is also seen in several other models that are part of the ACCMIP ensemble as discussed in Young et al. (2018). The exclusion of SNPm in EMEP model (Fig. 2: EMEP_SNPm – magenta line) didn't substantially affect the surface ozone concentrations over the receptor regions (maximum difference of ~ 1 ppbv from EMEP – blue line in Fig. 2), as the continental ozone predominantly had contributions from land-based local emission sources (see Appendix).

3. Results

3.1. Surface ozone seasonal cycle

In this section we discuss the role of international ship NOx emissions from various marine regions in the monthly mean surface ozone seasonal cycle simulated over various receptor regions as shown in Fig. 1c. Although only the grid points with availability of TOAR observations was considered for evaluation in section 2.2, we analyse the simulated ozone over the entire receptor region in this section. In subsections subsections 3.1.1 and 3.1.2, we discuss the contributions to the seasonal cycle using the NOx-tagging and combined-tagging approaches respectively, and in subsection 3.1.3 we discuss the potential impact of perturbing ship emissions at various marine regions in altering the seasonal cycle of surface ozone over the receptor regions.

3.1.1. NOx-tagged contributions

In the top panels of Figs. 3–5 the seasonal cycle of monthly mean surface ozone concentration (in ppbv) simulated in CAM-Chem for year 2010 ($O_3^{TOT(NOxT)}$) is shown as stacked contributions from various tagged NO_x emission regions/sectors in the NOx-tag-Base simulation ($O_3^{Tag(NOxT)}$; see Table 3) over various receptor regions considered in our study. This $O_3^{TOT(NOxT)}$ typically shows peaks during spring and summer months. The springtime peak typically has O_3 concentrations of ~35-45 ppb over the selected receptor regions, which are ~10 ppbv larger than the preceding winter months. This is mainly associated with large contributions from the natural component ($O_3^{NAT(NOxT)}$; ~15-20 ppb (40 %)), predominantly by the stratosphere-troposphere exchange (Figs. S2–S7; Monks, 2000) and from the remote land-anthropogenic component ($O_3^{REM(NOxT)}$; ~10-15 ppb (20 %)) usually due to long range transport of ozone mainly driven by continental outflow (HTAP, 2010; Cooper et al., 2010; Han et al., 2018). The local anthropogenic contributions are also relatively larger during spring compared to winter months. This component peaks during the summertime contributing up to ~20 ppbv (~60 %) essentially leading to the summertime peak in

Fig. 3. Seasonal cycle of surface ozone simulated in the NOx-tag-Base simulation over North American HTAP Tier 2 regions considered in our study (in ppbv). Top: NOx-tagged contributions to total surface mean ozone from various tagged components as indicated. Bottom: Contributions from various tagged Marine regions' ship NOx emissions to the "Shipping" component shown in the top panels. See supplement for the detailed contributions from various tags within the "Natural" and "Remote Land Anthropogenic" components shown here (Fig. S2) and the relative contributions (in %; Fig. S5) of the tags to the total surface ozone.

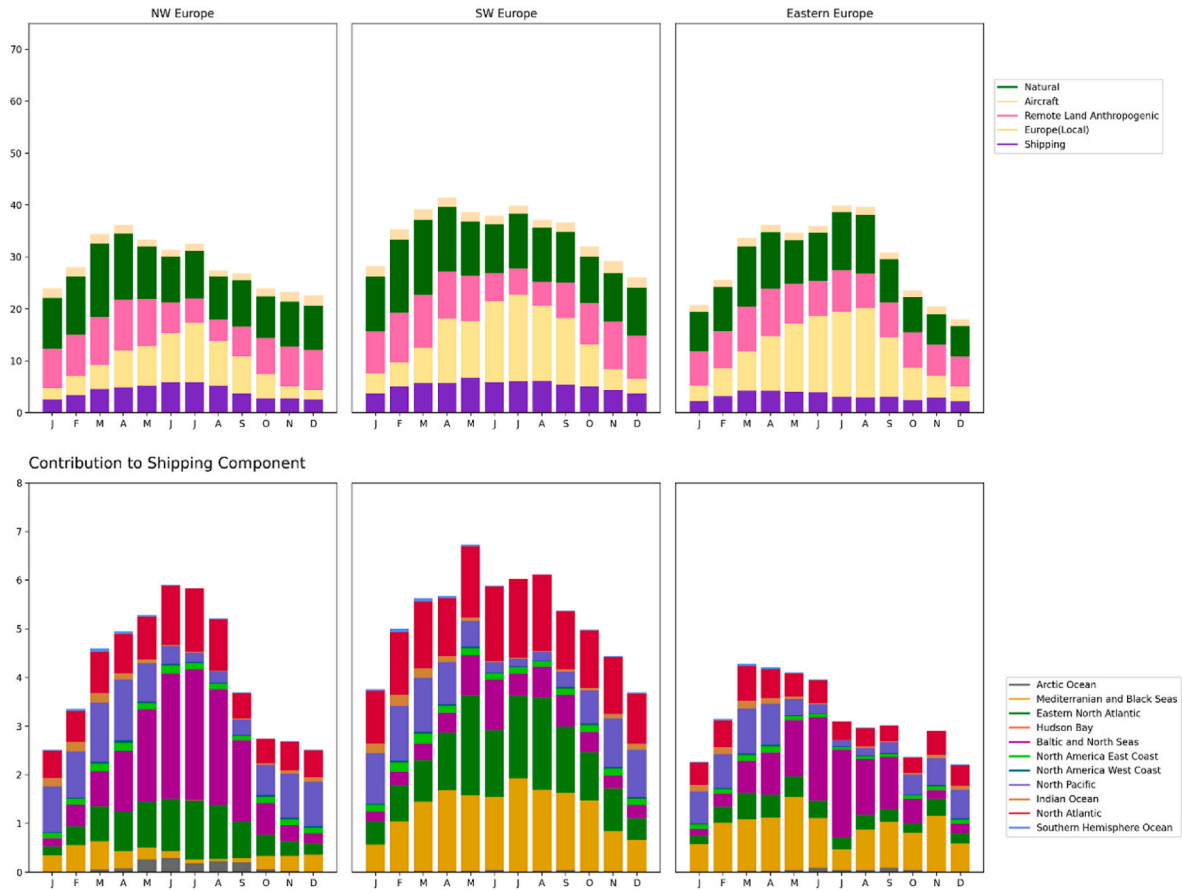

Fig. 4. Same as Fig. 3 but for European receptor regions (in ppbv). See supplement for the detailed contributions from various tags within the "Natural" and "Remote Land Anthropogenic" components shown here (Fig. S3) and the relative contributions (in %; Fig. S6) of the tags to the total surface ozone.

$O_3^{TOT(NOxT)}$ due to availability of sunlight and larger temperatures resulting in faster reaction rates and more biogenic RC emissions. The magnitude of contributions from aircraft NOx sources ($O_3^{AIR(NOxT)}$) are generally small (up to 3 ppbv) and remain fairly constant throughout the year over North American and European receptor regions.

Ship NOx emissions could also be considered as a remote source contributing to ozone concentrations over land regions. We show the ship NOx contribution ($O_3^{SHP(NOxT)}$) in the violet-coloured bottommost bars in the top panels of Figs. 3–5, and as annual means in Table 4. The disaggregated contributions from individual marine regions to $O_3^{SHP(NOxT)}$ is shown in the bottom panels corresponding to that receptor region. It is expected that, similar to other remote land-anthropogenic contributions discussed above, the ship NOx contribution may also peak during the spring and dip during summer. This is generally true over the North American receptor regions (Fig. 3; top panels: bottommost purple bars). However, over a few European and East Asian receptor regions (Figs. 4 and 5), $O_3^{SHP(NOxT)}$ peaks during summertime (consistent with Butler et al., 2020). The reason for this is due to a large summertime contribution by NO_x emissions from nearby marine regions.

For example, over NW Europe (Fig. 4; bottom panels), large summertime contributions are from the nearby NAL, BNS and ENA marine regions (summing up to ~4.5 ppb (16 %); leading to summertime peak in $O_3^{SHP(NOxT)}$), and smaller summertime contributions are from other remote marine regions (NPA, MBC etc.; 0.47 ppb (1.45 %)). The largest contribution during winter and spring to surface ozone over NW Europe interestingly is from NPA (~1.5 ppb (4 %)), which is a marine region very far from Europe. This is because of a large hemispheric signal from in $O_3^{NPA(NOxT)}$ during winter, as shown in Supplementary Fig. S8. Similarly, SW and Eastern Europe have large summertime contributions from NAL, ENA and MBC which are nearby marine regions (2 ppb (5 %)), but much smaller contributions from other marine regions. Over East Asian receptor regions (Fig. 5; bottom panel), the ship NO_x contribution from the Northern Pacific marine region ($O_3^{NPA(NOxT)}$), which is the nearby source region, is the largest and peaks during summertime (~5 ppb (17.5 %)). Contributions from all the other marine regions are small (less than 3 %), especially during the summertime.

As noted earlier, $O_3^{SHP(NOxT)}$ does not show a summertime peak contribution over North American receptor regions. The contributions to this component from nearby marine regions peak during summer (consistent with the feature also simulated over Europe and East Asia as noted above), however, these contributions are smaller than the contributions from remote marine regions that peak during spring. For example, SE US has larger contribution from nearby NAE and NAL marine regions (~1.5 ppb (4 %)) and smaller contributions from other remote marine regions during summer (less than 0.2 ppb) compared to other seasons. However, a cascading contribution from both nearby (e.g. $O_3^{NAE(NOxT)}$ and $O_3^{NAL(NOxT)}$) and larger contribution from remote (e.g. $O_3^{NPA(NOxT)}$) marine regions during April (each contributing up to 1 ppb) has led to a predominant springtime peak rather than a summertime peak. In contrast, NE US does not show a strong summertime peak form nearby marine regions possibly due to the influence of strong westerlies transporting the pollutants from these marine emission sources (such as NAE) eastward and away from the continent. Since the contributions from nearby marine region (that mainly include ECAs) ship NOx components are predominant both during summer and springtime, we note that the consideration of mitigating emissions from

Fig. 5. Same as Fig. 3 but for East Asian receptor regions (in ppbv). See supplement for the detailed contributions from various tags within the "Natural" and "Remote Land Anthropogenic" components shown here (Fig. S4) and the relative contributions (in %; Fig. S7) of the tags to the total surface ozone.

Table 4
Annual mean values of simulated surface ozone over the receptor regions considered in our study. The first three columns after the receptor region names, show the ozone (in ppb) simulated by CAM4-Chem ($O_3^{TOT(NOxT)}$), EMAC ($O_3^{TOT(Comb)}$) and EMEP ($O_3^{No-Tag-Base}$) models in their respective BASE simulations (as summarized in Table 1). The next two columns show the ship-tagged ozone (absolute values expressed in ppb) contributing to the total ozone simulated by CAM4-Chem ($O_3^{SHP(NOxT)}$) and EMAC ($O_3^{SHP(Comb)}$) in their BASE simulations respectively. The last two columns show the relative contribution by ship-tagged ozone CESM and EMAC to the total ozone (in %).

Receptor region	$O_3^{TOT(NOxT)}$ (ppb)	$O_3^{TOT(Comb)}$ (ppb)	$O_3^{No-tag-Base}$ (ppb)	$O_3^{SHP(NOxT)}$ (ppb)	$O_3^{SHP(Comb)}$ (ppb)	$\left(\frac{O_3^{SHP(NOxT)}}{O_3^{TOT(NOxT)}}\right) * 100$ (%)	$\left(\frac{O_3^{SHP(Comb)}}{O_3^{TOT(Comb)}}\right) * 100$ (%)
NW US	36.59	39.78	36.1	3.2	2.82	8.75	7.08
SW US	41.49	49.23	40.22	3.06	3.14	7.37	6.39
SE US	35.15	44.99	38.06	2.96	3.21	8.42	7.12
NE US	33.11	36.82	35.91	2.05	2.14	6.2	5.81
E. Canada	29.72	33.65	28.7	2.77	2.3	9.31	6.84
NW Europe	28.73	30.09	29.7	4.11	2.83	14.29	9.42
SW Europe	35.24	38.3	36.22	5.28	4.13	14.97	10.79
Eastern Europe	30	31.23	32.44	3.21	2.58	10.71	8.27
Korea	30.13	33.73	37.09	3.34	3.34	11.08	9.91
Japan	35.16	40.44	37.42	4.92	4.52	14.01	11.17
Mean	33.5	37.83	35.19	3.49	3.1	10.511	8.28
Median	34.13	37.56	36.16	3.205	2.985	10.01	7.695
Standard Deviation	3.78	5.75	3.52	0.94	0.72	2.9	1.82

these nearby sources is essential to reduce both the springtime peak (to a small extent) and the summertime peak (to a relatively large extent) in surface ozone over the receptor regions considered in our study. The mitigation of emissions from remote marine regions can also be considered for the reduction of springtime peak in surface ozone.

The contributions of ship NO_x emissions from Arctic, Indian and Southern Oceans, and from Hudson Bay are very small, as the emission magnitude (Fig. S1) is either too small or the region itself is too far from the regions considered in our study. The only noticeable contribution from $O_3^{ARC(NOxT)}$ is during the summer months over NW Europe by up to 0.3 ppbv (Fig. 4: left-bottom panel). We simulate $O_3^{IDO(NOxT)}$ contribution of up to 0.2 ppbv mainly during the non-summer months over most of receptor regions considered in our study.

3.1.2. Combined-tagged contributions

As stated in section 2.2.2, this combined-tagged approach attributes the contribution of both NOx and RC emissions from a given emission sector/region to the simulated ozone. Here an average of the relative proportion of the tagged NOx and RC ozone precursors from any given emission sector defines the production and loss rates of tagged ozone (eq. (1)). This implies, when one of the precursors (either NO_x or RC) represented by the tagged source categories has little or no emissions, the role of the other component is going to be considerably smaller than what would otherwise be simulated when only that particular precursor (NOx-tagged or RC-tagged) is tagged. For example, the methane sector (categorized as CH4 tag in our combined-tagged simulations; see Table 2) doesn't emit any NOx. When applied to equation (1), the NO_y proportion component would be very small (mainly emanating from decomposition of reservoir species such as peroxy-acyl nitrate) and approximately half of the RC proportion component would effectively be considered to calculate the methane-tagged ozone production, leading to simulating approximately only half of what would be simulated from an exclusively RC-tagged simulation. However, note that the combined tagging approach is non-linear, which also includes a HOx tagging scheme (Rieger et al., 2018) where feedback mechanism between NOx-HOx-O3 components occur.

In Fig. 6a and d, we present the combined-tagged contributions to the surface ozone (absolute and relative) simulated over NE US as an example for discussion (see supplement, as indicated in the title for Fig. 6, for the results over other receptor regions). We discuss these combined-tagged contributions in comparison with the NOx-tagged contributions shown in Fig. 6b and e. The main features in the seasonal cycle of contributions from tagged ozone components noted above are also seen in the NOx-tag-Base simulation: spring and summertime peaks in surface ozone contributed mainly by natural/remote and local anthropogenic NOx sources respectively, as shown in both the absolute (Fig. 6b) and relative (Fig. 6e) contributions. Nevertheless, these NOx-tagged contributions quantitatively vary compared to the Combined-tagged contributions discussed earlier. We show the differences in the contributions of the tagged components between the two simulations (Fig. 6c and f). Since the total ozone simulated using these two methods are performed in two different models: NOx-tag-Base in CAM-Chem and Comb-tag-Base in EMAC model (Table 1), differences in the simulated surface ozone (black line in Fig. 6c) are expected. We therefore emphasize our discussion on the differences of the relative contributions of tagged components, expressed with the units: "%-points" (Fig. 6f). Since CH4 component isn't simulated in the NOx-tag-Base simulation, we only plot the relative contribution by CH4 component in the Comb-

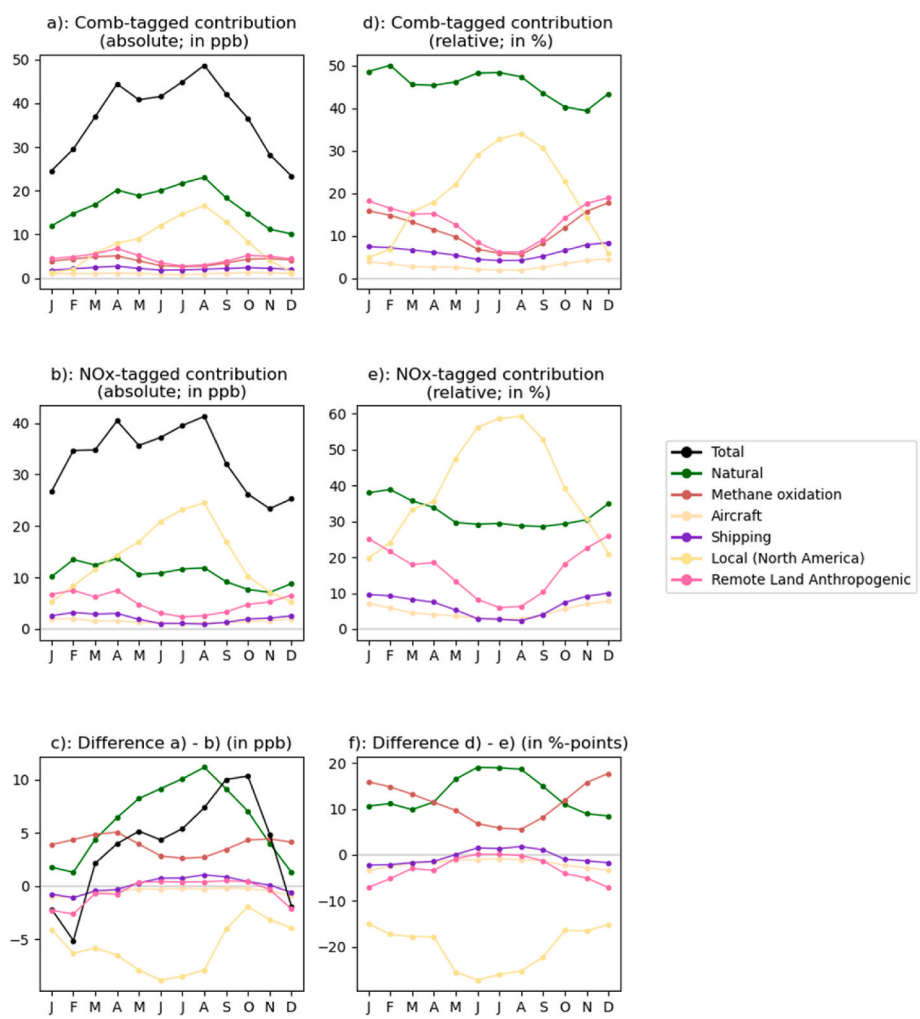

Fig. 6. All quantities shown here are seasonal cycles simulated over NE US. For the results over other receptor regions, see supplementary figures as indicated in the brackets next to the panel description in this text. These supplementary figures also show the disaggregated contributions to the Natural, Remote Land Anthropogenic and Shipping components for all receptor regions analysed in our study. **a)** (S9-S11) Surface ozone and it's contributing tagged components simulated in the Comb-tag-Base simulation ($O_3^{Tag(Comb)}$) (in ppbv). **b)** (S2-S4) Surface ozone and it's contributing tagged components simulated in the NOx-tag-Base simulation ($O_3^{Tag(NOxT)}$) (in ppbv) **c)** (S15-S17) Difference between the quantities (in ppbv) shown in a) and b). **d)** (S12-S14) Relative contribution of the tagged components to total ozone simulated in the Comb-tag-Base simulation (in %) **e)** (S5-S7) Relative contribution of the tagged components to total ozone simulated in the NOx-tag-Base simulation (in %) **f)** (S18-S20) Difference between the quantities (in %-points) shown in d) and e).

tag-Base simulation in Fig. 6f that shows the difference in relative contributions. The sum of all of the lines in Fig. 6f showing the differences in the relative contributions would become zero, indicating that a net positive difference would be compensated by an equal net negative difference.

The Natural component shows the largest positive difference (up to 20 %-points) during the summertime and is mainly contributed by the biogenic component (Figs. S18–S20: third row), as this also includes the contribution from biogenic RC emissions in the Comb-tag-Base simulation. Since a large amount of biogenic RCs are emitted during summer and contribute to ozone formation, their inclusion in equation (1) leads to a larger proportion of biogenic precursor emissions contributing to surface ozone compared to the inclusion of only biogenic/soil NOx (as in the NOx-tagged simulation, which is relatively small). The Local anthropogenic component shows the largest negative difference especially during summer months, indicating a much smaller contribution when anthropogenic emissions of both NOx and RC and considered in equal proportions. This is because, the proportion of anthropogenic RC emissions contributing to the total RC emissions (~22 %) is much smaller compared to the proportion of anthropogenic NOx emissions contributing to the total NOx emissions (~72 %), as noted in Nalam et al. (2025). Further, local anthropogenic NOx predominantly tends to react with biogenic RCs during the summer months. Therefore, while the NOx-tagging approach attributes the predominant local ozone to anthropogenic NOx, the combined-tagging approach attributes the local ozone production partially to the anthropogenic sector (leading to the negative difference; yellow line in Fig. 6f) and partially to the natural sector (largely biogenic RC, leading to the positive difference; green line shown in Fig. 6f and Figs. S18–S20).

Similarly, it may be expected that the difference in the relative contributions of shipping component also be large and negative, as the amount of RC emitted from ships is very small (less than 2 % of global RC) compared to the amount of NOx (up to 10 % of global NOx). In our study however, we simulate negative differences that are smaller than 5 %-points, and also some small positive differences during summer months. This could have several reasons, as not only the tagged shipping production terms differ between the approaches, but also the respective loss terms (see eq. (14) in Grewe et al., 2017), which may lead to longer lifetimes of the tagged ozone from shipping in the combined approach. Another reason could also be a larger amount of ozone simulated over ocean grid cells being simulated in the EMAC model (Comb-tag-Base simulation; compared to NOx-tag-Base simulation using CAM-Chem), that gets transported to the land grid cells. We may also notice in Figs. S12–S14: bottom row, that the generally small ozone contributing marine regions such as ARC, HBY, SHO etc show larger relative contribution by up to 0.2 % even during the winter months. We therefore recommend further studies implement different tagging methods within the same model so that a coherent comparison of the tagging methods and contributions from the tagged components can be obtained. The disaggregated contribution from nearby marine regions to the shipping component in the difference in relative contributions in Fig. 6f (Figs. S18–S20) show largest negative differences of 2.5-5 %-points. During winter and springtime, CH4 component contributes the largest positive (up to 18 %; Fig. 6f) differences in the relative contributions and is compensated by the negative differences in the relative contributions from anthropogenic components (aircraft, shipping, local and remote land anthropogenic). Considering the annual mean, we find that the relative contribution from the ship-tagged component in the combined-tagged simulation (last column in Table 4) is smaller than in the NOx-tagged simulation (penultimate column in Table 4) over every receptor regions by ~1-5 %-points. Although the simulated absolute or relative contribution from the tagged marine regions in some cases may be of similar magnitude for both the NOx-tagged and combined-tagged attribution methods, a careful chemical interpretation is necessary given the differences between the two methods.

3.1.3. Perturbation approach

As described in section 2.2.3, we perform perturbation simulations for 15 % NOx emissions reduction in the EMEP model for each individual marine region, and all marine regions as a whole (described in section 2.2.4). The seasonal cycle in potential impact/scaled response (calculated using equation (2)) of ship NOx emission perturbation from individual marine regions are stacked up and shown in Fig. 7. We express this sum of scaled responses to perturbation in individual marine regions as $\Sigma O_3^{Mreg(Pert)}$ for the sake of discussion.

Over most North American receptor regions (SE US being the exception), we notice a smaller impact from NOx perturbation over individual marine regions during summer compared to that in spring. This feature is consistent with the simulated NOx-tagged ($O_3^{SHP(NOxT)}$; Fig. 3) and combined-tagged ($O_3^{SHP(Comb)}$; Fig. S9) contributions from individual marine regions discussed in section 3.1.1, as the response to perturbation at nearby marine regions which peaks during summer is much smaller compared to the response to remote marine region perturbation that peaks during springtime (Fig. 3: bottom panels). For example, $O_3^{NAW(Pert)}$ over NW US and SW US is ~0.2 ppb larger during the summer months compared to the winter months, as NAW is the nearby marine region.

Over European receptor regions, we notice varying signs of the impacts for various marine regions' NOx perturbations. During the summer months, all responses show positive signs indicating that an increase in NOx emissions through perturbation leads to increase in ozone concentration. However, over the winter and spring months in some cases, the responses show a negative sign (eg. $O_3^{BNS(Pert)}$ is up to −0.1 ppb over NW and Eastern Europe during the non-summer months; consistent with Jonson et al., 2020) indicating a decrease in ozone concentration. This is mainly a scaled response to ship NOx perturbation over BNS marine region, and to a smaller extent from other nearby sources such as ENA and MBC over SW Europe. This small negative scaled response is a result of ozone loss in a NOx-saturated or RC-limited regime for ozone production. Usually, this regime occurs in the wintertime, as less sunlight is available to photolyze NO_2 to form ozone, effectively leading to an eventual loss of ozone through titration (reaction R3). This titration/negative-attribution feature in the behaviour of ozone SRRs can only be simulated using the perturbation approach, as the change in ozone in the RC-limited regime is simulated due to changes in NOx emissions. When averaging over a receptor region, there can be a compensating behaviour with some grid cells showing ozone decreases due to titration, while others showing ozone increase, resulting in an overall small positive response to perturbation in nearby sources such as ENA ($O_3^{ENA(Pert)}$) during winter. Consistent with the tagged contributions (bottom panels in Fig. 4 ($O_3^{NPA(NOxT)}$) discussed in earlier subsections, we simulate large wintertime response (up to 0.3 ppb) from ship NOx perturbation to the NPA region ($O_3^{NPA(Pert)}$) over European receptor regions.

Over East Asian receptor regions, the only nearby marine source region is NPA, as no other near-coast marine regions/ECAs around the East Asian coastline have been defined in our study (see section 2.3). This is why the response to ship NOx perturbation over NPA is the only predominant response over both South Korea and Japan. This response peaks during the summertime over both receptor regions (up to 2 ppb), consistent with the feature in the tagged contributions. During the spring and wintertime however, the NPA ship NOx perturbation leads to a negative scaled response (up to 0.2 ppb) in surface concentration over South Korea (but not over Japan) due to titration.

We may also notice from Fig. 7 to the height of the grey bars (scaled response to perturbation in ship NOx emissions over all marine regions simultaneously ($O_3^{Ship(Pert)}$)), is not exactly equal to the height of the adjacently stacked multicolored bars (sum of scaled responses to perturbation in ship NOx emissions over individual marine regions ($\Sigma O_3^{Mreg(Pert)}$)) during most months. This inequality is due to non-linearity in the ozone chemistry: the extent of ozone response is different from the extent of NOx perturbation (Grewe et al., 2010; Wu

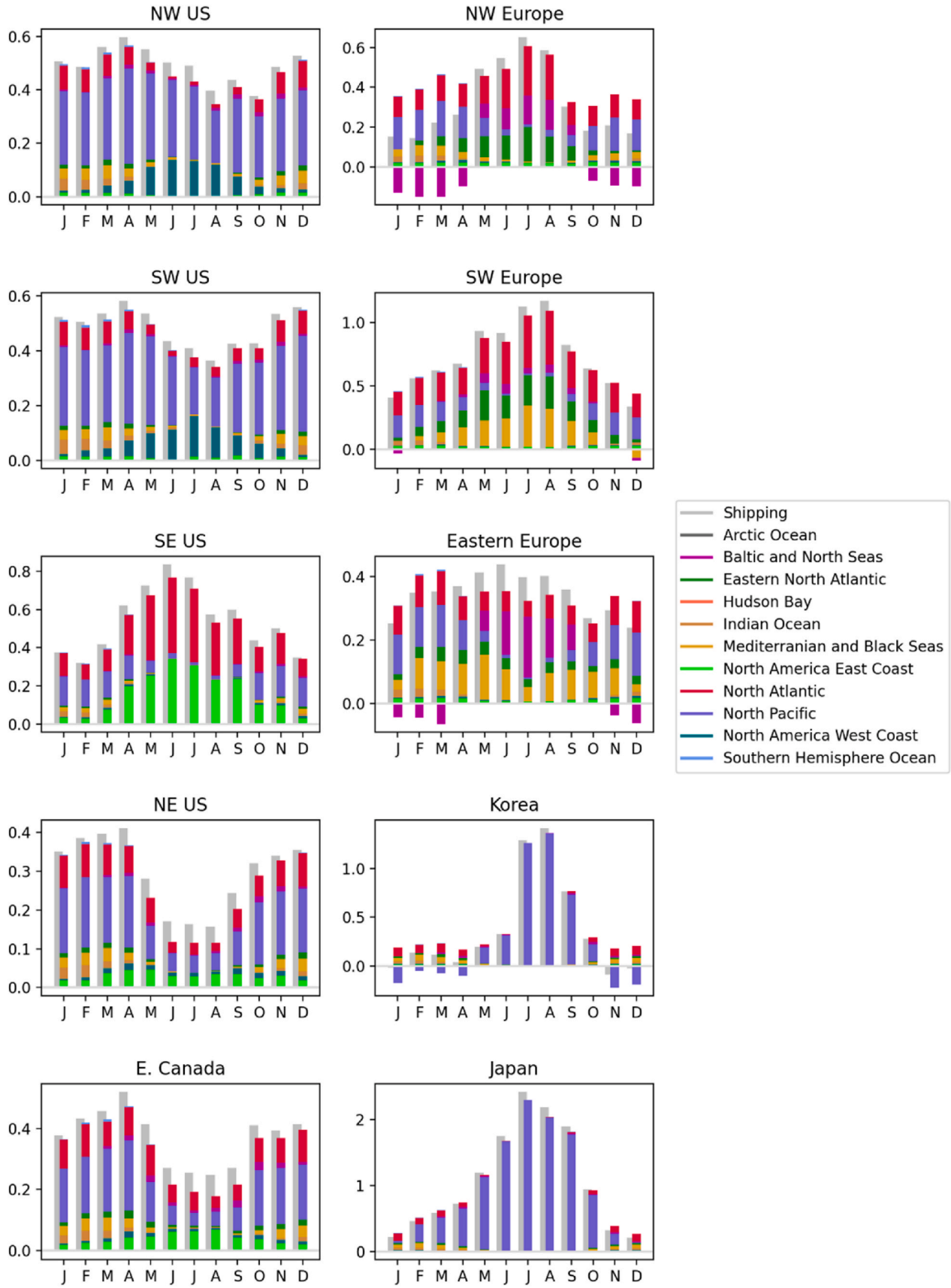

Fig. 7. Scaled responses to ship NOx perturbation (in ppbv) over various marine regions (see Fig. 1a) simulated by EMEP model, shown as coloured stacks representing the scaled responses to ship NOx perturbation over individual marine regions ($O_3^{Mreg(Pert)}$), calculated as explained in section 2.1.3. Also shown is the scaled response to perturbation in ship NOx over all marine regions simultaneously (grey bar adjacent to the coloured stacks: $O_3^{SHP(Pert)}$). Responses are shown over all the receptor regions considered in our study (Fig. 1c).

et al., 2009). Several factors can lead to this non-linear behaviour in ozone response; these include changes in ozone production efficiency (OPE) and NOx sensitivity regime that is induced by perturbation. NOx becomes more efficient at producing ozone when less NOx is emitted, since there are much fewer radical terminations leading to more NOx being able to produce ozone. In case of the perturbation method, the NOx emitted from various sources in the BASE and the PERTURBED simulations have different OPE: specifically, the NOx emitted in the PERTURBED simulations is smaller and much more efficient at producing ozone than in the BASE simulation. Since the absolute amount of NOx perturbation in each of our PERTURBED simulations (No-tag-Ship and No-tag-Mreg*) is different, we can expect inherent differences in the ozone responses between the individual and simultaneous marine region perturbations.

Emission perturbation can also induce a change in the sensitivity regime of ozone production. For example, Park et al. (2024) show that the inclusion of shipping emissions (100 % ship perturbation) can lead to a regime transition from NOx-limited to RC-limited and simulate an ozone titration signal over inland regions. In our study however, the extent of perturbation is small (15 %) resulting in a smaller chance of a drastic regime change and associated non-linearities, as suggested in previous studies (eg. Hoor et al., 2009; Grewe et al., 2012 etc.).

The EMEP simulations for the results discussed above in this subsection included the "ShipNOx" parameterization (SNPm). In this parameterization, only 50 % of the NOx emitted from ships could produce ozone while the remaining NOx are emitted as pseudo-species that have a lower O_3 generation potential. The inclusion/exclusion of SNPm represents the lower/upper limit of the effect of NOx emissions from ships, as mentioned in section 2.2.3 and in Jonson et al. (2020) (see Appendix A1 for elaborate discussion). The main effect of excluding SNPm in the Base simulations is that there is slightly larger ozone simulated by only 0.1 ppbv (less than 5 %) over receptor regions. The scaled response to perturbation in ship NOx emissions over all marine regions simultaneously, is also slightly larger (by up to 0.5 ppbv) when SNPm is excluded.

3.2. Global shipping perturbation responses: explaining compensating feedbacks through the tagging approach

In this section we compare the scaled responses to simultaneous ship NOx emission perturbation over all marine regions performed in all 3 models considered in our study (see section 2.2.4 and Table 1), with the tagged contribution from shipping simulated in the BASE simulations (NOx-tag-Base and Comb-tag-Base). This comparison between the tagged contributions ($O_3^{TAG(NOxT)}$ and $O_3^{TAG(Comb)}$) in the BASE simulations and the scaled responses in the tagged components ($O_3^{TAG(Pert-NOxT)}$ and $O_3^{TAG(Pert-Comb)}$) to ship emission perturbation can help us track the compensating feedbacks leading to the differences in the attributed quantities. Table 4 shows the annual mean surface ozone simulated in the BASE simulations along with the ship-tagged absolute and relative contributions. Table 5 shows the total ozone and the ship-tagged component scaled responses to the ship NOx perturbations. Both tables also show the summary statistics (mean, median and standard deviation) calculated across the selected receptor regions.

From the seasonal cycle in scaled responses in Fig. 8 and annual means in Table 5 (first three columns), we note that the scaled responses to ship perturbation in all three models ($O_3^{TOT(Pert-NOxT)}$: Orange line for CAM-Chem; $O_3^{TOT(Pert-Comb)}$: light green line for EMAC; and $O_3^{Ship(Pert)}$: blue line for EMEP) considered in our study are of similar magnitude (~0.5-1.5 ppb), and are smaller than the magnitude of tagged contribution from shipping in the tagged BASE simulations($O_3^{SHP(NOxT)}$: red line; $O_3^{SHP(Comb)}$: dark green line; Table 4: ~2-5 ppb) over every receptor region during nearly all months. $O_3^{Ship(Pert)}$shows a regular pattern in the response, with spring and/or summertime peaks in seasonal cycle over most receptor regions considered in our study. The responses from CAM-Chem and EMAC ($O_3^{TOT(Pert-NOxT)}$ and $O_3^{TOT(Pert-Comb)}$) however show noisy responses with large spikes in the seasonal cycle. The contributing responses from the tagged components are also of a similar noisy nature (Figs. S21–S26). The reasons are unknown at this point and shall be addressed in further studies. Despite these discrepancies pointed out for CAM-Chem and EMAC, all three models simulate a similar magnitude of scaled response to 15 % perturbation in global shipping NOx emission, over most receptor regions. The EMEP response is slightly larger (up to 2 ppbv) when SNPm is excluded as seen in the magenta line of Fig. 8, reflecting a larger sensitivity when more NOx can potentially form ozone (see Appendix A(ii) for further discussion related to this).

A closer look at the tagged contributions to the surface ozone response shows a larger response from the ship-tagged component, but a compensating negative response from other tagged sources such as land based anthropogenic and natural tagged sources (Figs. 9 and 10). There is an apparent larger compensating response from remote land-based anthropogenic (pink line) components compared to the local component (pale yellow line). This could possibly be due to noisy behavior in the seasonal cycle responses, as noted above, from individual regional anthropogenic components contributing to the remote land-based anthropogenic component that accumulate to form an overall response that ends up being larger than the response from the local component (Figs. S21–S23: second row).

Table 5
Annual mean values of simulated scaled responses of surface ozone to perturbation in ship NOx emissions. These responses are shown over the receptor regions considered in our study. The first three columns after the receptor region names, show the scaled ozone responses (in ppb) simulated by CAM4-Chem ($O_3^{TOT(Pert-NOxT)}$), EMAC ($O_3^{TOT(Pert-Comb)}$) and EMEP ($O_3^{Ship(Pert)}$) models and are calculated using equations (4)–(6) respectively. The next two columns show the responses in ship-tagged ozone (in ppb) simulated by CAM4-Chem ($O_3^{SHP(NOxT)}$) and EMAC ($O_3^{SHP(Comb)}$) in their BASE simulations respectively. The last two columns show the ratio between the ship-tagged ozone response and total surface ozone response in CESM and EMAC.

Receptor region	$O_3^{TOT(Pert-NOxT)}$ (ppb)	$O_3^{TOT(Pert-Comb)}$ (ppb)	$O_3^{Ship(Pert)}$ (% of $O_3^{No-tag-Base}$) (ppb (%))	$O_3^{SHP(Pert-NOxT)}$ (ppb)	$O_3^{SHP(Pert-Comb)}$ (ppb)	$\frac{O_3^{SHP(Pert-NOxT)}}{O_3^{TOT(Pert-NOxT)}}$ ratio	$\frac{O_3^{SHP(Pert-Comb)}}{O_3^{TOT(Pert-Comb)}}$ ratio
NW US	1.03	0.56	0.92 (2.55)	2.99	1.94	2.91	3.48
SW US	1.42	0.8	0.89 (2.21)	3.55	2.18	2.51	2.74
SE US	1.19	0.57	0.87 (2.29)	2.9	1.6	2.44	2.83
NE US	1.14	0.6	0.55 (1.53)	2.64	1.55	2.32	2.59
E. Canada	1.17	0.82	0.7 (2.43)	3.03	2.39	2.59	2.91
NW Europe	1.22	0.74	0.71 (2.39)	3.05	2.35	2.51	3.18
SW Europe	0.8	0.54	1.24 (3.42)	2.5	2.64	3.14	4.93
Eastern Europe	1.23	1.13	0.63 (1.94)	2.62	2.49	2.13	2.2
Korea	1.15	0.75	0.58 (1.56)	2.56	2	2.23	2.67
Japan	0.97	0.49	1.68 (4.48)	2.52	1.71	2.59	3.48
Mean	1.13	0.7	0.88 (2.48)	2.84	2.09	2.54	3.1
Median	1.16	0.67	0.79 (2.33)	2.77	2.09	2.51	2.87
Standard Deviation	0.16	0.18	0.33 (0.84)	0.32	0.37	0.29	0.72

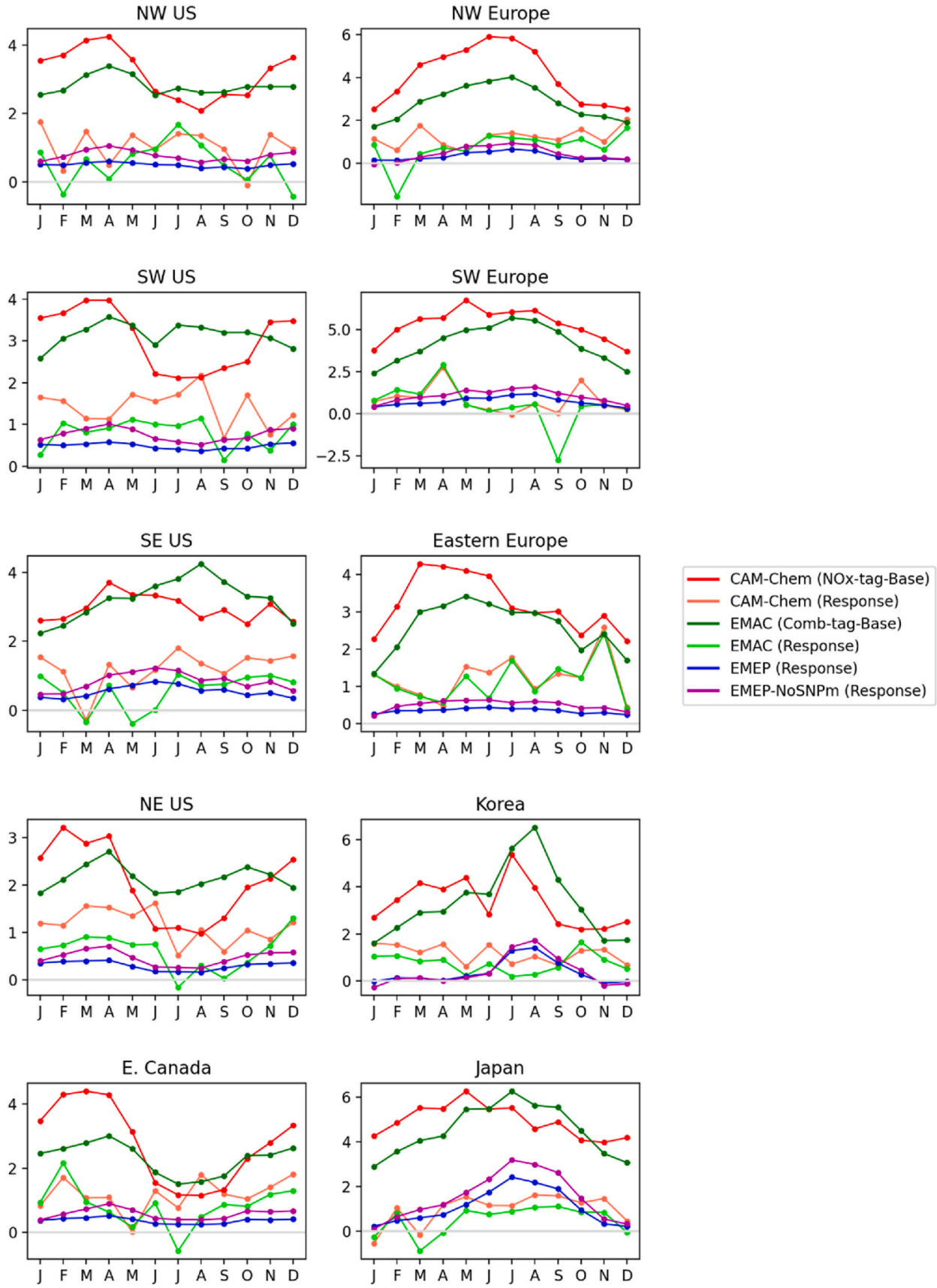

Fig. 8. Seasonal cycle in the tagged absolute contributions from the shipping component to the total surface ozone (in ppbv) in the NOx-tag-Base (Dark Red line: $O_3^{SHP(NOxT)}$) and Combined-tag-Base (Dark Green line: $O_3^{SHP(Comb)}$) simulations over the regions considered in our study. Also shown are the scaled responses to ship-NOx perturbations (orange line: $O_3^{TOT(Pert-NOxT)}$, light green line: $O_3^{TOT(Pert-NOxT)}$, blue line: $O_3^{Ship(Pert)}$ and magenta line: $O_3^{NoSNPm(Pert)}$) in each of the models considered in our study.

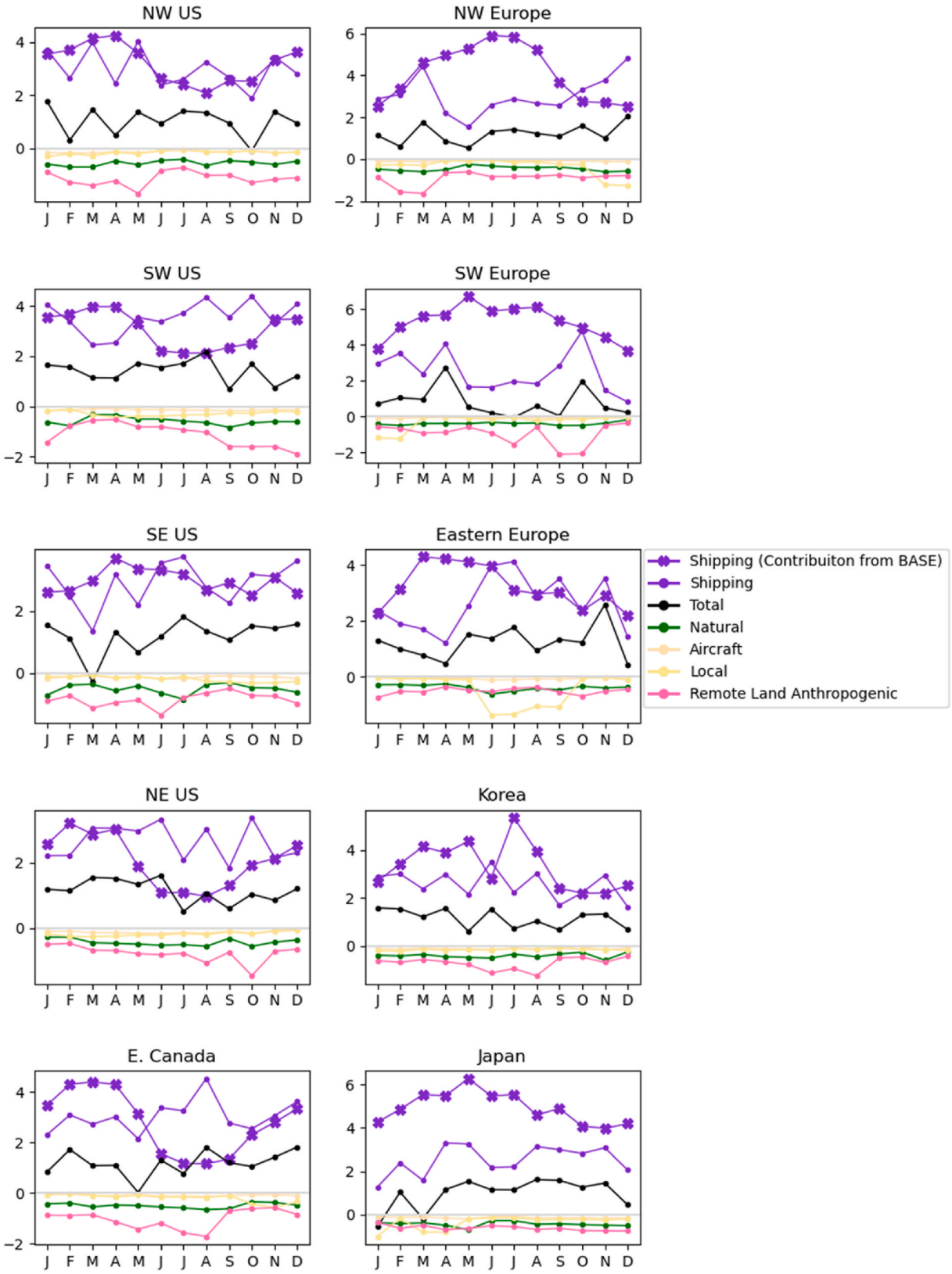

Fig. 9. Scaled responses of surface ozone and various NOx-tagged components (in ppb) to the Ship perturbation ($O_3^{TAG(Pert-NOxT)}$). The responses are shown over the receptor regions considered in our study. Also shown is the ship-tagged component in the NOx-Tag-Base simulation (purple line with crossed marker: $O_3^{SHP(NOxT)}$). Note that the "Local" and "Remote Land Anthropogenic" components are different for each of the receptor regions (Eg: Local component for European receptor regions is the Europe tag; Remote Land Anthropogenic component is the sum of all land region tags in Fig. 1b other than Europe). See Supplementary Figs. S21–S23 for the disaggregated contributions to the natural, remote land anthropogenic and shipping components shown here.

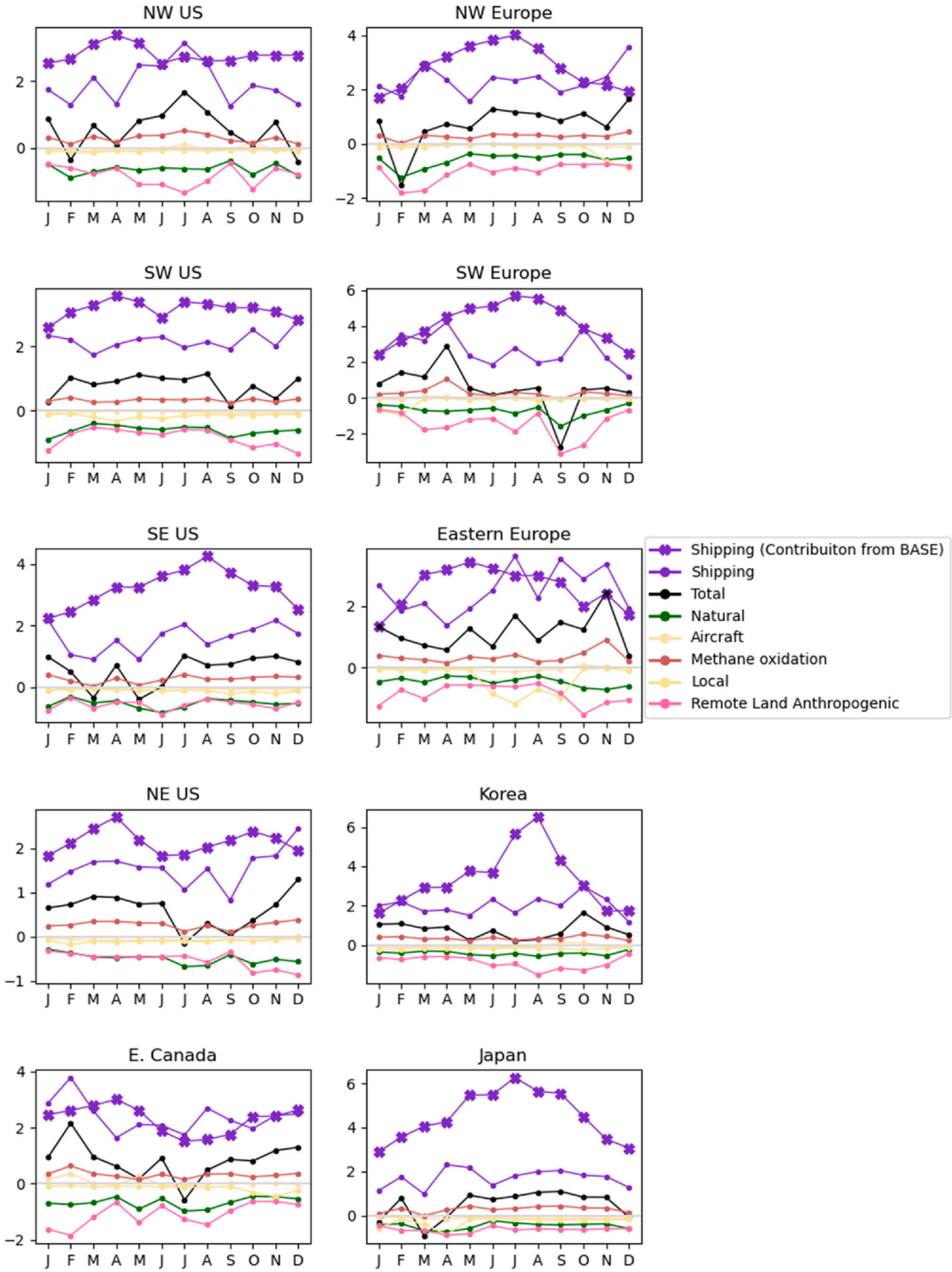

Fig. 10. Same as Fig. 9 but for Combined-tagged components. Also shown is the ship component in the Comb-Tag-Base simulation (purple line with crossed marker: $O_3^{SHP(Comb)}$). See Supplementary Figs. S24–S26 for the disaggregated contributions to the natural, remote land anthropogenic and shipping components shown here.

Table 6
Summary of the results from the attribution methods considered in our study, along with their benefits and limitations.

	NOx-tagging	Combined-tagging	Perturbation
Application/ notes	**Direct attribution** to ship **NOx** only	- Attributes to **both NOx and RC emissions** (giving equal weightage) from shipping sector. - - Attributed value smaller than that of NOx-tagged attribution	- Attributes the **sensitivity/impact** of emission changes - Simulates **negative attribution** due to titration - Scaled response is generally smaller than the tagged contribution
Benefits	**Exclusive** contribution from **NOx-only** sources	Both **NOx and RC sectoral attribution** within the **same simulation**	- **Negative attribution** possible - Incorporating tagged chemical mechanism not required
Limitation	- **Separate simulation** required O_3 to attribute RC sources such as CH4. - Can't simulate negative attribution due to titration.	- **Only partial** ship-NOx attribution possible - Can't simulate negative attribution due to titration.	- Can't simulate share of individual emission sectors/regions - Individual attributions don't add up to the total value due to **non-linearity**

The reason for these compensating contributions in the non-marine tagged sources is the smaller ozone production from inland NOx sources due to larger competition of the perturbed NOx from shipping emissions in forming ozone (eg. Nalam et al., 2025). We illustrate these changes in ozone production in response to perturbation by tabulating the changes in the annual mean tropospheric ozone burden (TOB) and the tagged components contributing to the overall non-tagged TOB change (Table S2 and the text therein). The TOB attributed to ship NOx in our NOx-tagged simulation increases in response to the ship NOx perturbation by ~3.01 Tg O_3, which is compensated by a reduction in the contribution from non-ship anthropogenic and natural tagged NOx sources by ~1.44 TgO_3, thereby leading to an overall TOB increase of ~1.55 TgO_3. Our combined-tagged simulation also shows a similar feature with ship-tagged contribution increasing by ~2.29 TgO_3 while the non-ship-tagged contributions decreased by ~1.68 TgO_3. The contribution from CH4 tag in our combined-tagged simulation also increases but to smaller extent (~0.47 TgO_3), leading to an overall change in non-tagged TOB is ~1.08 TgO_3. Essentially, the ozone production from non-ship-tagged emission sources decreases as a result of perturbation, thereby leading to an overall non-tagged TOB change to be smaller than the TOB attributed to ship emissions.

The response in the ship-tagged component ($O_3^{SHP(Pert-NOxT)}$ and $O_3^{SHP(Pert-Comb)}$) is somewhat comparable to the ship-tagged contribution in the BASE simulation ($O_3^{SHP(NOxT)}$ and $O_3^{SHP(Comb)}$). The compensating contribution discussed above leads to the overall surface ozone responses ($O_3^{TOT(Pert-NOxT)}$ and $O_3^{TOT(Pert-Comb)}$; black lines) to be smaller (by 2-3 ppb; Figs. 9 and 10) than the ship-tagged responses (purple lines with crossed markers), consistent with the compensating reductions in the ozone productivity as noted in Table S2. In other words, the annual mean ship-tagged responses in surface ozone are 2-3 times larger than the responses in the non-tagged responses as shown in the last 2 columns of Table 5.

In particular regarding the responses in combined-tagged components (Fig. 10), the response from methane tag ($O_3^{CH4(Pert-Comb)}$) also shows a positive response similar to, but with a much smaller magnitude (up to 0.5 ppb over all receptor regions), compared to that of the response from Shipping tag ($O_3^{SHP(Pert-Comb)}$). This positive response is because in the remote open ocean where ship NOx emissions are present, the main source of RC for ozone formation is from methane oxidation (which is a well-mixed gas), thereby making shipping and methane oxidation components respond in a coherent manner, consistent with the positive TOB change for CH4 tag shown in Table S2 (eg. Eyring et al., 2007; Hoor et al., 2009; Butler et al., 2020).

4. Conclusions: summary, limitations and future scope

In this study, we quantify the effect that ship NOx emissions can have on surface ozone concentrations over various continental regions simulated in GACMs. We attribute simulated surface ozone to NOx emissions over various marine regions (both emission control areas and major ocean basins; Fig. 1a) using three methods of ozone source attribution: NOx-tagging, Combined-tagging and perturbation. A concise comparison of the three methods is shown in Table 6 and explained briefly below.

Using the NOx-tagging attribution method, we estimate ~2-5 ppb (6-15 %; Table 4) contribution from $O_3^{SHP(NOxT)}$ component (sum of all individual marine region components) to the simulated surface ozone over the receptor regions considered in our study. The summertime peak in $O_3^{SHP(NOxT)}$, is due to larger ozone contribution from nearby marine regions. Over the winter and springtime, the contributions from these nearby sources reduce due to smaller availability of sunlight for the photochemical production of ozone, thereby favouring larger relative contributions from remote marine sources. The combined-tagged approach attributes only 5-10 % relative contribution from ship-tagged component ($O_3^{SHP(Comb)}$) to total simulated ozone, which is a smaller relative contribution compared to the NOx-tagged approach (by ~1-5 %-points; Table 4: last two columns), due to an equally weighted small contribution of RC emitted from ships taken into consideration (Eq. (1)). The main features of the seasonal cycle in ship contribution calculated by combined-tagged approach are similar to that calculated by NOx-tagged attribution approach.

Unlike the tagging attribution approach mentioned above that calculates the *contribution* from ship emissions to the simulated surface ozone, perturbation approach calculates the *sensitivity/impact/response* to changes in ship emissions at individual marine regions. Consistent with the tagged attribution results, we simulate a peak summertime response in surface ozone for ship NOx perturbation over nearby marine regions. During the non-summer months over some regions, we simulate a negative response in surface ozone to the ship NOx perturbation over nearby marine regions by up to 0.2 ppb (eg. BNS perturbation response over NW Europe; Fig. 7: top right panel) due to ozone titration in a NOx-saturated ozone sensitivity regime. The simulation of this negative attribution feature is only possible using this perturbation method. Small differences between the sum of responses to perturbating ship NOx over individual marine regions and the response to perturbing all marine regions simultaneously (likely due to non-linearities in ozone chemistry) have also been noted.

The responses to ship NOx perturbation simulated in all three models in our study (0.5-1.7 ppb; median: ~2.3 %; Table 5) are nearly always smaller than the ship tagged contributions (2-5.3 ppb; median: ~7.7 % combined-tagged, ~10 % NOx-tagged; Table 4; Fig. 8) in the respective BASE simulations. We further perform tagged simulations with ship NOx perturbations in order to further explain the differences in the ship NOx contribution derived in the tagged BASE simulations and the potential impact derived using the perturbation method. We find that the response from the ship-tagged component in both NOx-tagged and Combined-tagged simulations is ~2.3-5 times larger than the non-tagged ozone response (Table 5: last two columns) and is comparable to the ship-tagged contribution in the respective BASE simulations (Figs. 9 and 10). This smaller response from non-tagged ozone to ship NOx perturbation is due to a decrease in ozone production from components tagged with inland sources (natural, local anthropogenic and remote land anthropogenic), resulting in a compensating negative

response. These compensating changes in ozone production from various tagged sources illustrate the non-linearities in the atmospheric chemistry, leading to the quantitative differences in the ozone attributed to ship emissions using various attribution methods. In the Combined-tagged simulation, the response from the methane-tagged component is small but positive which is in coherence with the response from the ship-tagged component as RC from methane oxidation is the predominant source of RC for the production of ozone in remote pristine locations such as open oceans.

Our study attempting to understand the applications of various approaches discussed above, uses three different models with different resolutions and each using different boundary conditions, except the emissions from international shipping (Table 1). We can thus expect inherent differences in the simulated surface ozone by the three models. Moreover, the simulation results are presented only for 1 year of simulation. Despite this limitation, we believe that the key messages from our study summarized above, are qualitatively robust and are likely to hold, even with several other years of simulation or when all three attribution approaches are incorporated within the same model. Nevertheless, we recommend further studies incorporate different attribution techniques within the same model, prescribe consistent boundary conditions across the attribution simulations and also perform the simulation for several years in order to firmly establish both the qualitative and quantitative differences between the attributed quantities.

While we only attribute the monthly mean surface ozone concentration, follow-up studies could also attribute the policy relevant ozone metrics such as maximum daily 8-h running mean (MDA8), sum of ozone MDA8 over 35 ppb (SOMO35), Peak Season Ozone etc. and understand the source-receptor relationship during extreme ozone episodes (Eg. Mertens et al., 2020, Lupascu et al., 2022; Hu et al., 2024; Ansari et al., 2025). This attribution could also be extended to other pollutants such as NO_2, SO_2, PM etc., and to effects such as ozone and nitrogen deposition (e.g., Karl et al., 2019), and radiative forcing (e.g., Mertens et al., 2024). Our study could also be extended to understanding the air quality implications of international shipping in various future scenarios. While our study attributed continental surface ozone to ECAs close to Europe and North American coastline, further studies could also attribute ozone to emissions from the domestic ECAs near the East Asian coastline (eg. Liu et al., 2018).

As noted in section 3.2, the combination of tagging and perturbation can be used to track the factors leading to non-linearities in the source-receptor relationship of ozone and its precursor emission sources. The seasonal cycle in scaled response to ship NO_x perturbation in our tagged simulations using CAM-Chem and EMAC has been noisy, in contrast with the scaled response simulated by EMEP that shows a smooth seasonal cycle with spring/summer peaks (Fig. 9). In future studies we will attempt to diagnose the reason for this behaviour and arrive at a better and consistent seasonal cycle in the simulated scaled response. Nevertheless, from our simulations we identified a consistent compensating negative response in non-ship-tagged components leading to the magnitude of scaled response in surface ozone to ship NOx perturbation in all the three models to be smaller than the ship-tagged contribution in the BASE simulations (see section 3.2). We recommend further studies perform tagged perturbation simulations for individual marine regions too, along with perturbing all marine regions simultaneously. This would enable us to have better insights into the extent to which the contributions from marine regions change with individual regional perturbations.

Since with changing emissions the ozone production from various NOx sources would also change, tagged perturbation simulations would provide crucial insight into the extent of ozone production change from each of the tagged sources. This has direct relevance for estimating the expected changes in future ozone under NOx emission reductions and would require performing tagged perturbation simulations (eg. For methane perturbation in Butler et al., 2020 or for future scenario in Mertens et al., 2024). Similarly, we recommend tagged sensitivity simulations that include/exclude SNPm and enhance our understanding by accounting for the changes in contributions from tagged components to simulated surface ozone. Comparisons could also be done with other types of attribution methods such as the direct decoupling method (Mathur et al., 2022), or to tag ozone molecules according to the location of their formation (e.g., Sudo and Akimoto, 2007) as opposed to tagging by the identity of their precursor emission source used in our study. Finally, we recommend that care should be taken by both scientific and policy-making communities while expressing or discussing the SRRs i.e. the pollutant concentration attributed to a particular emission source: tagging method communicates the *contribution* of a particular emission source, while perturbation method communicates the *potential impact/scaled response to emission perturbation*.

CRediT authorship contribution statement

Aditya Nalam: Writing – original draft, Visualization, Methodology, Formal analysis, Conceptualization. **Mariano Mertens:** Writing – review & editing, Methodology. **Volker Grewe:** Writing – review & editing, Methodology. **Willem van Caspel:** Writing – review & editing, Methodology. **Jan Eiof Jonson:** Writing – review & editing, Methodology. **Tim Butler:** Writing – review & editing, Supervision, Conceptualization.

Declaration of competing interests

The authors declare that they have no known competing financial interests or personal relationships that could have appeared to influence the work reported in this paper.

Acknowledgements

AN acknowledges the funding from the Bundesministerium für Bildung und Forschung (grant no. 01US1701). Open Access Funding provided by Freie Universität Berlin.

MM acknowledges funding from the German Ministry of Research, Technology and Space (BMFTR) under the projects MAREMIS (01DP21008B) and IMPAC^{2}T (01LN2207A). This work uses resources of the Deutsches Klimarechenzentrum (DKRZ) granted by its Scientific Steering Committee (WLA) under project ID bd1063. Further, datasets provided by MESSy via the DKRZ data pool were used.

For the simulations performed using the EMEP MSC-W model, IT infrastructure in general was available through the Norwegian Meteorological Institute (MET Norway). Some computations were performed on resources provided by UNINETT.

Sigma2 – the National Infrastructure for High Performance Computing and Data Storage in Norway (grant nos. NN2890k and NS9005k). This work has been funded in part by the EMEP Trust Fund.

Appendix A. Results related to exclusion of ShipNOx parameterization in EMEP model

In the EMEP simulations discussed in section 2.2.3 (No-tag-Base, No-tag-Ship and No-tag-MReg*) as main EMEP results in our paper, we activate the "ShipNOx" parameterization (SNPm; see Jonson et al., 2020). In this configuration, 50 % of the NOx emitted from ships are emitted as pseudo-species called ShipNOx and undergo simple reactions such as $ShipNO_x + OH \longrightarrow HNO3$, or $ShipNO_x \longrightarrow HNO_3$. These ShipNOx pseudo species (that are 50 % of the emitted NOx from ships) that form HNO_3 (which has a smaller potential to form ozone compared to NOx, and tends to get deposited rapidly), while only the remaining 50 % of the emitted NO_x can form ozone. This SNPm is recommended for inclusion so that the over-estimation of ozone formation due to instant dilution of NOx emitted from ships into coarse resolution grid cells of GACMs. We include SNPm only in the EMEP model simulations mentioned above and not in the EMAC and CAM-Chem simulations.

In the additional EMEP sensitivity simulations: NoSNPm-Base and NoSNPm-Ship, we exclude this SNPm parameterization. Therefore, all of the emitted NOx from ships can potentially form ozone. In other words, these NoSNPm simulations emit more reactive nitrogen from ships than the ones mentioned in the previous paragraph.

In this section, we compare (i) the simulated surface ozone in the Base simulations (No-tag-Base and NoSNPm-Base), and (ii) the scaled responses in surface ozone to perturbation in ship NOx emissions over all marine regions simultaneously. In case of NoSNPm, the scaled response (expressed as $O_3^{NoSNPm(Pert)}$) is calculated similar to eq. (5), as shown below

$$O_3^{NoSNPm(Pert)} = (O_3^{NoSNPm-Base} - O_3^{NoSNPm-Ship}) * 100/15$$

The simulated ozone values (both in Base and scaled responses) in the simulations with and without SNPm represent the lower and upper limits of the effect of NOx emitted from ships. The differences indicate the range in these limits. In other words, these differences show the effect of excluding SNPm, thereby including relatively more NOx emissions that could potentially form ozone.

A (i) Comparison of surface ozone simulated in the Base simulations

Fig. A1 shows an increase of up to 3 ppb over ocean grid cells and up to 2 ppb over land grid cells (mainly close to the coastline). When averaged over the receptor regions considered in our study (Fig. A2), the increase is only up to 1 ppb as the averaging is performed over inland regions which are relatively less sensitive to emission perturbations over ocean grid cells. This difference is really small (less than 5 %) compared to the original Base value of surface ozone is each of the simulations (up to 50 ppb in Base simulations; Fig. 2).

A (ii) Comparison of scaled responses to perturbation in ship NOx emissions over all marine regions simultaneously

Fig. A3 shows a larger scaled response to ship NOx emission perturbation when SNPm is excluded from the simulations. The difference in the scaled responses is larger over the ocean grid cells (up to 4 ppbv) and small over the land regions (up to 2 ppbv). When averaged over the receptor regions, the simulated scaled response in up to 0.5 ppbv larger when SNPm is excluded (Fig. 8). The larger scaled response due to exclusion of SNPm reflects a larger sensitivity when more NOx emissions can potentially form ozone.

We also notice a smaller scaled response (negative difference of up to 4 ppbv) over North-western coast of Europe and Northeastern coast of China. This is because of those regions being NOx saturated, thereby leading to more ozone titration due to the exclusion of SNPm or inclusion of more reactive NOx emissions.

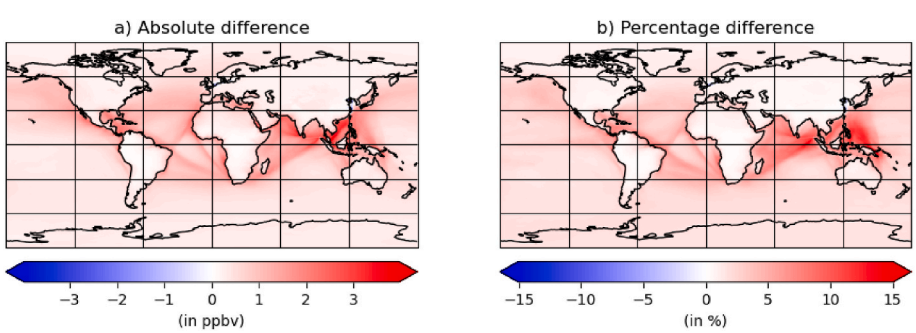

Fig. A1. a) Absolute and b) Percentage difference in the annual mean surface ozone simulated in NoSNPm-Base and No-tag-Base simulations. This difference illustrates the effect of exclusion of SNPm in the EMEP simulations and quantifies the range in the upper and lower limits of the effect of NOx emitted from ships on surface ozone mixing ratio.

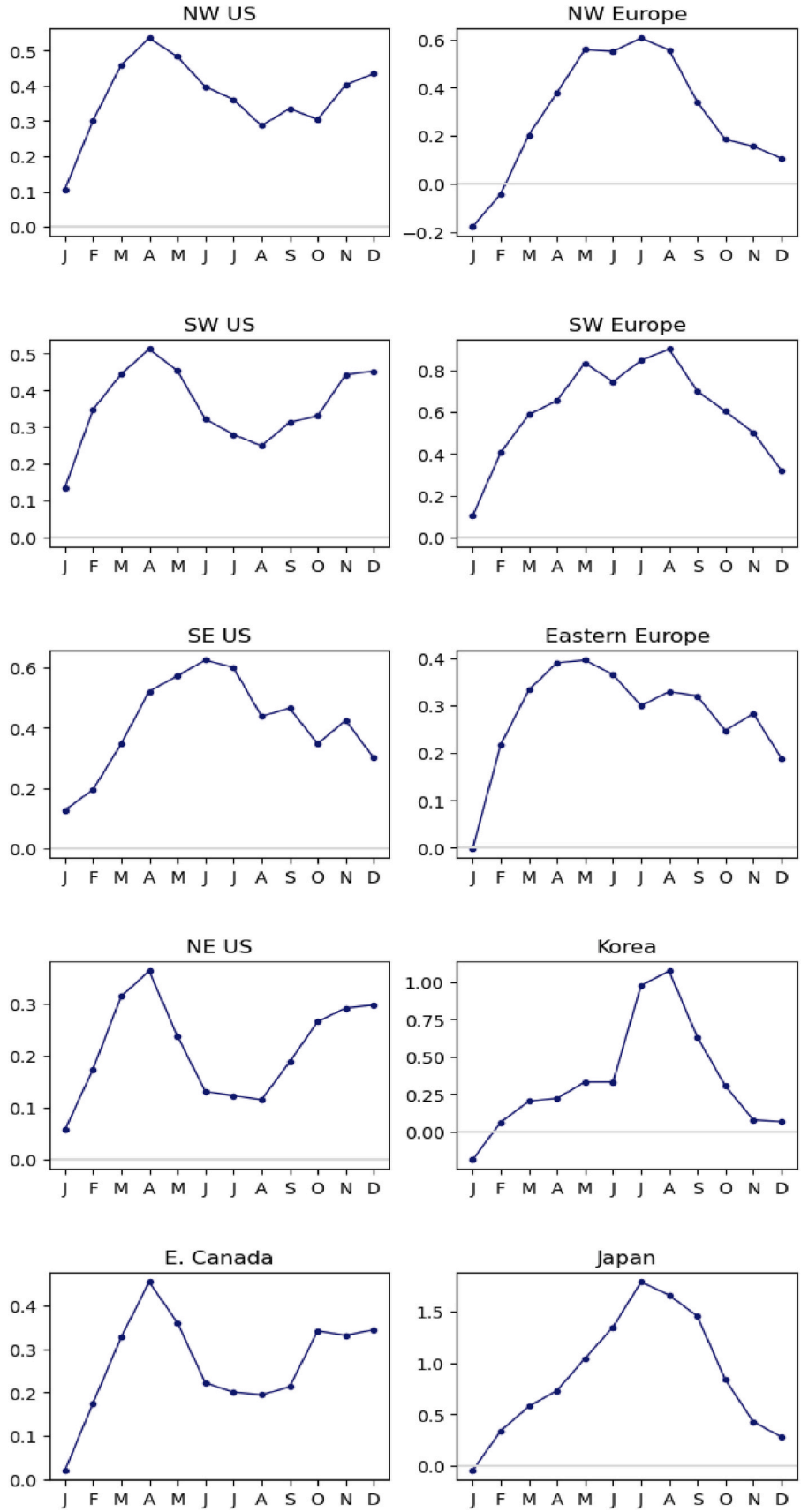

Fig. A2. Same as Fig. A1a but shown as a surface ozone seasonal cycle (in ppbv) and averaged over receptor regions shown in Fig. 1c.

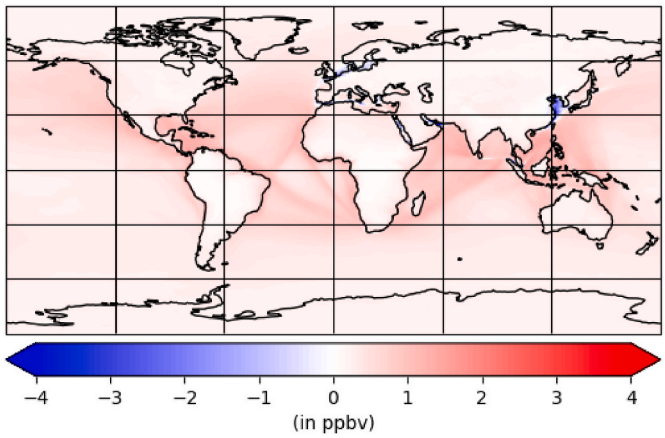

Fig. A3. Difference in the annual mean scaled response in surface ozone to all marine region NOx perturbation simulated without and with SNPm included ($O_3^{NoSNPm\,(Pert)}$ - $O_3^{Ship(Pert)}$).

Appendix A. Supplementary data

Supplementary data to this article can be found online at https://doi.org/10.1016/j.atmosenv.2026.122328.

Data availability

Data will be made available on request.

References

Ansari, T., Nalam, A., Lupascu, A., Hinz, C., Grasse, S., Butler, T., 2025. Explaining trends and changing seasonal cycles of surface ozone in North America and Europe over the 2000–2018 period: a global modelling study with NOx and VOC tagging. Atmos. Chem. Phys. 25, 16833–16876.

Avnery, S., Mauzerall, D.L., Liu, J., Horowitz, L.W., 2011. Global crop yield reductions due to surface ozone exposure: 1. year 2000 crop production losses and economic damage. Atmos. Environ. 45, 2284–2296.

Bergström, R., Hayman, G., Jenkin, M., Simpson, D., 2022. Update and Comparison of Atmospheric Chemistry Mechanisms for the Emep msc-w Model System. The Norwegian Meteorological Institute, Oslo, Norway emep.int/publ/reports/2022/MSCW technical 1 2022 640.

Butler, T., Lupascu, A., Coates, J., Zhu, S., 2018. TOAST1.0: tropospheric ozone attribution of sources with tagging for CESM 1.2. 2. Geosci. Model Dev. 11, 2825–2840.

Butler, T., Lupascu, A., Nalam, A., 2020. Attribution of ground-level ozone to anthropogenic and natural sources of nitrogen oxides and reactive carbon in a global chemical transport model. Atmos. Chem. Phys. 20, 10707–10731.

Chameides, W., Walker, J.C., 1973. A photochemical theory of tropospheric ozone. J. Geophys. Res. 78, 8751–8760.

Clappier, A., Thunis, P., Pirovano, G., Riffault, V., Gilardoni, S., Pisoni, E., Guerreiro, C., Monteiro, A., Dupont, H., Waersted, E., Hellebust, S., 2022. Source Apportionment to Support Air Quality Management Practices.

Cooper, O.R., Parrish, D., Stohl, A., Trainer, M., Nédélec, P., Thouret, V., Cammas, J.P., Oltmans, S., Johnson, B., Tarasick, D., et al., 2010. Increasing springtime ozone mixing ratios in the free troposphere over western North America. Nature 463, 344–348.

Crutzen, P.J., 1974. Photochemical reactions initiated by and influencing ozone in unpolluted tropospheric air. Tellus 26, 47–57.

Deckert, R., Jöckel, P., Grewe, V., Gottschaldt, K.-D., and Hoor, P.: A quasi chemistry-transport model mode for EMAC, Geosci. Model Dev., 4, 195–206. https://doi.org/10.5194/gmd-4-195-2011,2011.

Dee, D.P., Uppala, S., Simmons, A.J., Berrisford, P., Poli, P., Kobayashi, S., Andrae, U., Balmaseda, M., Balsamo, G., Bauer, d.P., et al., 2011. The ERA-interim reanalysis: configuration and performance of the data assimilation system. Q. J. R. Meteorol. Soc. 137, 553–597.

Emmons, L., Hess, P., Lamarque, J.F., Pfister, G., 2012. Tagged ozone mechanism for MOZART-4, CAM-Chem and other chemical transport models. Geosci. Model Dev. 5, 1531–1542.

Emmons, L.K., Schwantes, R.H., Orlando, J.J., Tyndall, G., Kinnison, D., Lamarque, J.F., Marsh, D., Mills, M.J., Tilmes, S., Bardeen, C., et al., 2020. The chemistry mechanism in the Community Earth System Model version 2 (CESM2). J. Adv. Model. Earth Syst. 12 e2019MS001882.

Franciscus, D., Keating, T., Hajime, A., 2011. Hemispheric Transport of Air Pollution 2010: Part A-tropospheric Ozone and Particulate Matter.

Galmarini, S., Koffi, B., Solazzo, E., Keating, T., Hogrefe, C., Schulz, M., Benedictow, A., Griesfeller, J.J., Janssens-Maenhout, G., Carmichael, G., et al., 2017. Coordination and harmonization of the multi-scale, multi-model activities HTAP2, AQMEII3, and MICS-Asia3: simulations, emission inventories, boundary conditions, and model output formats. Atmos. Chem. Phys. 17, 1543–1555.

Ge, Y., Solberg, S., Heal, M.R., Reimann, S., van Caspel, W., Hellack, B., Salameh, T., Simpson, D., 2024. Evaluation of modelled versus observed non-methane volatile organic compounds at european monitoring and evaluation programme sites in Europe. Atmos. Chem. Phys. 24, 7699–7729.

Granier, C., Darras, S., van Der Gon, H.D., Jana, D., Elguindi, N., Bo, G., Michael, G., Marc, G., Jalkanen, J.P., Kuenen, J., et al., 2019. The Copernicus atmosphere monitoring service global and regional emissions (April 2019 version). Copernicus Atmosphere Monitoring Service. Ph.D. thesis.

Grewe, V., Brunner, D., Dameris, M., Grenfell, J.L., Hein, R., Shindell, D., Staehelin, J., 2001. Origin and variability of upper tropospheric nitrogen oxides and ozone at northern mid-latitudes. Atmos. Environ. 35 (20), 3421–3433.

Grewe, V., Dahlmann, K., Matthes, S., Steinbrecht, W., 2012. Attributing ozone to NOx emissions: implications for climate mitigation measures. Atmos. Environ. 59, 102–107.

Grewe, V., Tsati, E., Hoor, P., 2010. On the attribution of contributions of atmospheric trace gases to emissions in atmospheric model applications. Geosci. Model Dev. 3, 487–499.

Grewe, V., Tsati, E., Mertens, M., Frömming, C., Jöckel, P., 2017. Contribution of emissions to concentrations: the TAGGING 1.0 submodel based on the Modular Earth Submodel System (MESSy 2.52). Geosci. Model Dev. 10, 2615–2633.

Han, H., Liu, J., Yuan, H., Zhuang, B., Zhu, Y., Wu, Y., Yan, Y., Ding, A., 2018. Characteristics of intercontinental transport of tropospheric ozone from Africa to Asia. Atmos. Chem. Phys. 18, 4251–4276.

Holmes, C., Prather, M., Vinken, G., 2014. The climate impact of ship NOx emissions: an improved estimate accounting for plume chemistry. Atmos. Chem. Phys. 14, 6801–6812.

Hoor, P., Borken-Kleefeld, J., Caro, D., Dessens, O., Endresen, O., Gauss, M., Grewe, V., Hauglustaine, D., Isaksen, I.S., Jöckel, P., et al., 2009. The impact of traffic emissions on atmospheric ozone and oh: results from quantify. Atmos. Chem. Phys. 9, 3113–3136.

Hu, F., Xie, P., Tian, X., Xu, J., Li, A., Lupaşcu, A., Butler, T., Hu, Z., Lv, Y., Zhang, Z., et al., 2024. Integrated analysis of the transport process and source attribution of an extreme ozone pollution event in Hefei at different vertical heights: a case of study. Sci. Total Environ. 906, 167237.

Huntrieser, H., Heland, J., Schlager, H., Forster, C., Stohl, A., Aufmhoff, H., Arnold, F., Scheel, H., Campana, M., Gilge, S., et al., 2005. Intercontinental air pollution transport from North america to Europe: experimental evidence from airborne measurements and surface observations. J. Geophys. Res. Atmos. 110.

Huszar, P., Cariolle, D., Paoli, R., Halenka, T., Belda, M., Schlager, H., Miksovsky, J., Pisoft, P., 2010. Modeling the regional impact of ship emissions on NOx and ozone levels over the eastern Atlantic and Western Europe using ship plume parameterization. Atmos. Chem. Phys. 10, 6645–6660.

IIASA, 2019. Global Emission Fields of Air Pollutants and GHGs. international institute for applied systems analysis (iiasa) eclipsev6b data. https://iiasa.ac.at/models-tools-data/global-emission-fields-of-air-pollutants-a (last access: February 2026).

Jalkanen, J.P., Johansson, L., Kukkonen, J., 2016. A comprehensive inventory of ship traffic exhaust emissions in the European sea areas in 2011. Atmos. Chem. Phys. 16 (1), 71–84.

Jöckel, P., Tost, H., Pozzer, A., Brühl, C., Buchholz, J., Ganzeveld, L., Hoor, P., Kerkweg, A., Lawrence, M.G., Sander, R., Steil, B., Stiller, G., Tanarhte, M., Taraborrelli, D., van Aardenne, J., Lelieveld, J., 2006. The atmospheric chemistry

general circulation model ECHAM5/MESSy1: consistent simulation of ozone from the surface to the mesosphere. Atmos. Chem. Phys. 6, 5067–5104. https://doi.org/10.5194/acp-6-5067-2006.

Jöckel, P., Tost, H., Pozzer, A., Kunze, M., Kirner, O., Brenninkmeijer, C.A.M., Brinkop, S., Cai, D.S., Dyroff, C., Eckstein, J., Frank, F., Garny, H., Gottschaldt, K.-D., Graf, P., Grewe, V., Kerkweg, A., Kern, B., Matthes, S., Mertens, M., Meul, S., Neumaier, M., Nützel, M., Oberländer-Hayn, S., Ruhnke, R., Runde, T., Sander, R., Scharffe, D., Zahn, A., 2016. Earth system chemistry integrated modelling (ESCiMo) with the modular Earth submodel system (MESSy) version 2.51. Geosci. Model Dev. 9, 1153–1200. https://doi.org/10.5194/gmd-9-1153-2016.

Jonson, J.E., Gauss, M., Schulz, M., Jalkanen, J.P., Fagerli, H., 2020. Effects of global ship emissions on European air pollution levels. Atmos. Chem. Phys. 20, 11399–11422.

Junge, C.E., 1962. Global ozone budget and exchange between stratosphere and troposphere. Tellus 14, 363–377.

Karl, M., Bieser, J., Geyer, B., Matthias, V., Jalkanen, J.P., Johansson, L., Fridell, E., 2019. Impact of a nitrogen emission control area (NECA) on the future air quality and nitrogen deposition to seawater in the Baltic sea region. Atmos. Chem. Phys. 19, 1721–1752.

Kerkweg, A., Sander, R., Tost, H., Jöckel, P., 2006. Implementation of prescribed (OFFLEM), calculated (ONLEM), and pseudo-emissions (TNUDGE) of chemical species in the modular Earth submodel system (MESSy). Atmos. Chem. Phys. 6 (11), 3603–3609.

Kilian, M., Grewe, V., Jöckel, P., Kerkweg, A., Mertens, M., Zahn, A., Ziereis, H., 2024. Ozone source attribution in polluted European areas during summer 2017 as simulated with MECO(n). Atmos. Chem. Phys. 24, 13503–13523. https://doi.org/10.5194/acp-24-13503-2024.

Kim, H.S., Kim, Y.H., Han, K.M., Kim, J., Song, C.H., 2016. Ozone production efficiency of a ship-plume: ITCT 2K2 case study. Chemosphere 143, 17–23.

Lamarque, J.F., Emmons, L.K., Hess, P.G., Kinnison, D.E., Tilmes, S., Vitt, F., Heald, C.L., Holland, E.A., Lauritzen, P.H., Neu, J., Orlando, J.J., 2012. CAM-chem: description and evaluation of interactive atmospheric chemistry in the community Earth system model. Geosci. Model Dev. 5 (2), 369–411.

Lawrence, M.G., Crutzen, P.J., 1999. Influence of NOx emissions from ships on tropospheric photochemistry and climate. Nature 402, 167–170.

Levy II, H., 1972. Photochemistry of the lower troposphere. Planet. Space Sci. 20, 919–935.

Li, P., Yang, Y., Wang, H., Li, S., Li, K., Wang, P., Li, B., Liao, H., 2023. Source attribution of near-surface ozone trends in the United States during 1995–2019. Atmos. Chem. Phys. 23, 5403–5417.

Liu, H., Jin, X., Wu, L., Wang, X., Fu, M., Lv, Z., Morawska, L., Huang, F., He, K., 2018. The impact of marine shipping and its DECA control on air quality in the Pearl River Delta, China. Sci. Total Environ. 625, 1476–1485.

Lupascu, A., Butler, T., 2019. Source attribution of European surface O_3 using a tagged O_3 mechanism. Atmos. Chem. Phys. 19, 14535–14558.

Lupascu, A., Otero, N., Minkos, A., Butler, T., 2022. Attribution of surface ozone to NOx and volatile organic compound sources during two different high ozone events. Atmos. Chem. Phys. 22, 11675–11699.

Malashock, D.A., DeLang, M.N., Becker, J.S., Serre, M.L., West, J.J., Chang, K.L., Cooper, O.R., Anenberg, S.C., 2022. Estimates of ozone concentrations and attributable mortality in urban, peri-urban and rural areas worldwide in 2019. Environ. Res. Lett. 17, 054023.

Mathur, R., Kang, D., Napelenok, S.L., Xing, J., Hogrefe, C., Sarwar, G., Itahashi, S., Henderson, B.H., 2022. How have divergent global emission trends influenced long-range transported ozone to North America? J. Geophys. Res. Atmos. 127 e2022JD036926.

McDuffie, E.E., Smith, S.J., O'Rourke, P., Tibrewal, K., Venkataraman, C., Marais, E.A., Zheng, B., Crippa, M., Brauer, M., Martin, R.V., 2020. A global anthropogenic emission inventory of atmospheric pollutants from sector-and fuel-specific sources (1970–2017): an application of the community emissions data system (CEDS). Earth Syst. Sci. Data 12, 3413–3442.

Mertens, M., Brinkop, S., Graf, P., Grewe, V., Hendricks, J., Jöckel, P., Lanteri, A., Matthes, S., Rieger, V.S., Righi, M., et al., 2024. The contribution of transport emissions to ozone mixing ratios and methane lifetime in 2015 and 2050 in the shared socioeconomic pathways (SSPs). Atmos. Chem. Phys. 24, 12079–12106.

Mertens, M., Grewe, V., Rieger, V.S., Jöckel, P., 2018. Revisiting the contribution of land transport and shipping emissions to tropospheric ozone. Atmos. Chem. Phys. 18, 5567–5588.

Molod, A., Takacs, L., Suarez, M., Bacmeister, J., 2015. Development of the GEOS-5 atmospheric general circulation model: Evolution from MERRA to MERRA2. Geosci. Model Dev. 8, 1339–1356.

Monks, P.S., 2000. A review of the observations and origins of the spring ozone maximum. Atmos. Environ. 34, 3545–3561.

Nalam, A., Lupascu, A., Ansari, T., Butler, T., 2025. Regional and sectoral contributions of NOx and reactive carbon emission sources to global trends in tropospheric ozone during the 2000–2018 period. Atmos. Chem. Phys. 25, 5287–5311.

Park, J., Mun, J., Kim, D., Lee, H.W., Kim, C.H., Lee, H.J., Jo, H.Y., Koo, J.Y., Choe, H., Jeon, W., 2024. Assessing the impact of shipping emissions on ozone concentrations in East Asia: insights from KORUS-AQ and SIJAQ 2021 campaign periods. Atmos. Environ. 320, 120339.

Price, C., Rind, D., 1992. A simple lightning parameterization for calculating global lightning distributions. J. Geophys. Res. Atmos. 97 (D9), 9919–9933.

Rieger, V.S., Mertens, M., Grewe, V., 2018. An advanced method of contributing emissions to short-lived chemical species (OH and HO_2): the TAGGING 1.1 submodel based on the modular earth submodel system (MESSy 2.53). Geosci. Model Dev. 11, 2049–2066.

Schultz, M.G., Schröder, S., Lyapina, O., Cooper, O.R., Galbally, I., Petropavlovskikh, I., Von Schneidemesser, E., Tanimoto, H., Elshorbany, Y., Naja, M., et al., 2017. Tropospheric ozone assessment report: database and metrics data of global surface ozone observations. Elem. Sci. Anth. 5, 58.

Simpson, D., Benedictow, A., Berge, H., Bergström, R., Emberson, L.D., Fagerli, H., Flechard, C.R., Hayman, G.D., Gauss, M., Jonson, J.E., et al., 2012. The EMEP MSC-W chemical transport model–technical description. Atmos. Chem. Phys. 12, 7825–7865.

Simpson, D., Tsyro, S., Wind, P., 2015. Updates to the EMEP MSC-W model, 2018 – 2019. In: Transboundary Particulate Matter, photo-oxidants, Acidifying and Eutrophying Components, EMEP Status Report 1/2015. The Norwegian Meteorological Institute, Oslo, Norway, pp. 129–136. https://emep.int/publ/reports/2015/EMEP_Status_Report_1_2015.pdf (last access: 7 July 2020).

Sindelarova, K., Markova, J., Simpson, D., Huszar, P., Karlicky, J., Darras, S., Granier, C., 2021. Copernicus Atmosphere Monitoring Service Global Biogenic Voc Emissions Version 3.0 (CAMS-GLOB-BIO v3. 0). ECCAD.

Sudo, K., Akimoto, H., 2007. Global source attribution of tropospheric ozone: Long-range transport from various source regions. J. Geophys. Res. Atmos. 112.

Tilmes, S., Lamarque, J.F., Emmons, L., Kinnison, D., Ma, P.L., Liu, X., Ghan, S., Bardeen, C., Arnold, S., Deeter, M., et al., 2015. Description and evaluation of tropospheric chemistry and aerosols in the community earth system model (CESM1. 2). Geosci. Model Dev. 8, 1395–1426.

Topic, T., Murphy, A.J., Pazouki, K., Norman, R., 2023. NOx emissions control area (NECA) scenario for ports in the north adriatic sea. J. Environ. Manag. 344, 118712.

van Caspel, W.E., Simpson, D., Jonson, J.E., Benedictow, A.M.K., Ge, Y., Di Sarra, A., Pace, G., Vieno, M., Walker, H., Heal, M., 2023. Implementation and evaluation of updated photolysis rates in the EMEP MSC-W chemical transport model using Cloud-J v7. 3e. Geosci. Model Dev. Discuss. (GMDD) 2023, 1–44.

Van der Werf, G.R., Randerson, J.T., Giglio, L., Collatz, G., Mu, M., Kasibhatla, P.S., Morton, D.C., DeFries, R., Jin, Y.v., van Leeuwen, T.T., 2010. Global fire emissions and the contribution of deforestation, savanna, forest, agricultural, and peat fires (1997–2009). Atmos. Chem. Phys. 10, 11707–11735.

Vinken, G.C., Boersma, K.F., Jacob, D.J., Meijer, E.W., 2011. Accounting for non-linear chemistry of ship plumes in the GEOS-Chem global chemistry transport model. Atmos. Chem. Phys. 11, 11707–11722.

Wang, H., Lu, X., Jacob, D.J., Cooper, O.R., Chang, K.L., Li, K., Gao, M., Liu, Y., Sheng, B., Wu, K., et al., 2022. Global tropospheric ozone trends, attributions, and radiative impacts in 1995–2017: an integrated analysis using aircraft (IAGOS) observations, ozonesonde, and multi-decadal chemical model simulations. Atmos. Chem. Phys. 22, 13753–13782.

Wang, X., Zhang, C., Gao, Y., Ji, X., Su, W., Liu, C., 2023. Satellite unravels recent changes in atmospheric nitrogen oxides emissions from global ocean shipping. J. Clean. Prod. 429, 139591.

Wiedinmyer, C., Kimura, Y., McDonald-Buller, E.C., Emmons, L.K., Buchholz, R.R., Tang, W., Seto, K., Joseph, M.B., Barsanti, K.C., Carlton, A.G., et al., 2023. The fire inventory from NCAR version 2.5: an updated global fire emissions model for climate and chemistry applications. Geosci. Model Dev. 16, 3873–3891.

Wu, S., Duncan, B.N., Jacob, D.J., Fiore, A.M., Wild, O., 2009. Chemical nonlinearities in relating intercontinental ozone pollution to anthropogenic emissions. Geophys. Res. Lett. 36.

Young, P.J., Naik, V., Fiore, A.M., Gaudel, A., Guo, J., Lin, M., Neu, J., Parrish, D., Rieder, H., Schnell, J., et al., 2018. Tropospheric ozone assessment report: assessment of global-scale model performance for global and regional ozone distributions, variability, and trends. Elem. Sci. Anth. 6, 10.